[24] G. J. Nau, P. Guilfoile, G. L. Chupp et al., "A chemoattractant cytokine associated with granulomas in tuberculosis and silicosis," *Proceedings of the National Academy of Sciences of the United States of America*, vol. 94, no. 12, pp. 6414–6419, 1997.

[25] S.-I. Inomata, N. Shijubo, S. Kon et al., "Circulating interleukin-18 and osteopontin are useful to evaluate disease activity in patients with tuberculosis," *Cytokine*, vol. 30, no. 4, pp. 203–211, 2005.

[26] M. Liu, S. Guo, J. M. Hibbert et al., "CXCL10/IP-10 in infectious diseases pathogenesis and potential therapeutic implications," *Cytokine and Growth Factor Reviews*, vol. 22, no. 3, pp. 121–130, 2011.

[27] M. Baggiolini, B. Dewald, and B. Moser, "Human chemokines: an update," *Annual Review of Immunology*, vol. 15, pp. 675–705, 1997.

[28] M. Ruhwald, M. Bjerregaard-Andersen, P. Rabna, J. Eugen-Olsen, and P. Ravn, "IP-10, MCP-1, MCP-2, MCP-3, and IL-1RA hold promise as biomarkers for infection with M. tuberculosis in a whole blood based T-cell assay," *BMC Research Notes*, vol. 2, article 19, 2009.

[29] D. Goletti, A. Raja, B. S. A. Kabeer et al., "Is IP-10 an accurate marker for detecting M. tuberculosis-specific response in HIV-infected persons," *PLoS ONE*, vol. 5, no. 9, Article ID e12577, 2010.

[30] N. P. Juffermans, A. Verbon, S. J. H. Van Deventer et al., "Elevated chemokine concentrations in sera of human immunodeficiency virus (HIV)-seropositive and HIV-seronegative patients with tuberculosis: a possible role for mycobacterial lipoarabinomannan," *Infection and Immunity*, vol. 67, no. 8, pp. 4295–4297, 1999.

[31] P. F. Barnes, J. M. Leedom, L. S. Chan et al., "Predictors of short-term prognosis in patients with pulmonary tuberculosis," *Journal of Infectious Diseases*, vol. 158, no. 2, pp. 366–371, 1988.

[32] A. M. Wengner, S. C. Pitchford, R. C. Furze, and S. M. Rankin, "The coordinated action of G-CSF and ELR + CXC chemokines in neutrophil mobilization during acute inflammation," *Blood*, vol. 111, no. 1, pp. 42–49, 2008.

[33] N. Mukaida, A. Harada, and K. Matsushima, "Interleukin-8 (IL-8) and monocyte chemotactic and activating factor (MCAF/MCP-1), chemokines essentially involved in inflammatory and immune reactions," *Cytokine and Growth Factor Reviews*, vol. 9, no. 1, pp. 9–23, 1998.

[34] Y. Zhang, M. Broser, H. Cohen et al., "Enhanced interleukin-8 release and gene expression in macrophages after exposure to Mycobacterium tuberculosis and its components," *Journal of Clinical Investigation*, vol. 95, no. 2, pp. 586–592, 1995.

[35] G. Akpek, "Hematologic findings in mycobacterial infections among immunosuppressed and immunocompetent patients," in *Tuberculosis*, M. M. Madkour, Ed., pp. 213–230, Springer, Berlin, Germany, 2004.

[36] F. Abebe and G. Bjune, "The protective role of antibody responses during *Mycobacterium tuberculosis* infection," *Clinical and Experimental Immunology*, vol. 157, no. 2, pp. 235–243, 2009.

506]
法中に発生した血液透析を要する急性腎不全症例の検討
学大学院医歯薬学総合研究科腎・免疫・内分泌代謝内科学[1],
大学大学院医歯薬学総合研究科慢性腎臓病対策腎不全治療学[2]
宏幸（たなべ　かつゆき）[1], 田中景子[1], 小松原基志[1],
史[1], 寺見直人[1], 中山和典[1], 綿谷博雪[1], 益田加奈[1],
子[1], 山成俊夫[2], 森永裕士[1], 杉山　斉[2], 槇野博史[1]

疾患に対する化学療法施行中に急性腎不全を発生することは稀
が，透析療法を要する症例は少なく，その病態は多様で，しば
断に苦慮する．ここ1年間に当院で化学療法中に急性腎不全を
透析療法の必要性から当科紹介となったのは9例で，6例は
腫瘍，3例が固形腫瘍であった．前者の腎不全は，いずれも原
再燃に伴って起こった．後者は（1）子宮体癌，（2）非小細胞
（3）神経膠腫であり，化学療法に関連した急性腎不全と考え，
ために血液透析を開始した．症例（1）はcarboplatinによる急
管壊死と判断し，維持透析を必要とした．症例（2）は
rumab投与中に発生したが，腎生検では半月体形成性腎炎を認
ステロイドに反応なく維持透析となった．症例（3）は
zolomide投与中に起こり，腎生検にて間質性腎炎の像を認め，
イドが奏功して透析を離脱した．

507]
により救命し得た薬剤性肝腎症候群の1例
島総合病院肝胆膵外科[1], JA広島総合病院消化器内科[2],
島総合病院救急・集中治療科[3]
彰彦（おおした　あきひこ）[1], 山口拓朗[1], 野中裕広[2],
生[3], 櫻谷正明[3], 佐々木秀[1], 吉田研一[3], 徳毛宏則[2],
志[1]

50歳代，男性．肝内胆管癌（T3N0M0Stage3）の診断で肝左
肝外胆管切除を伴うリンパ節郭清＋胆道再建術を施行．第6
39℃台の発熱を認め逆行性胆管炎を疑いTazobactam/
cillin（以下，TAZ/PIPC）の投与を開始．CTでは炎症の
指摘できず，その後も解熱せず炎症所見の改善に乏しいため
日にTAZ/PIPCからDoripenem（以下，DRPM）に変更した．
日よりD.Bil優位のT.Bil上昇を認め，以後T.Bilの上昇傾向
た．US，CT，MRIより胆管空腸吻合部の狭窄による閉塞性黄
外，薬剤性肝障害の可能性を考慮し第20病日DRPM投与を中
22病日にはT.Bil 32.3mg/dLまで上昇を認め，Cr 2.26mg/dL
害も出現したためCHDFを開始した．速やかにT.Bilは低下し
日にCHDFを終了した．それ以降はT.Bilも再上昇せず第43
軽快退院された．
肝腎症候群の原因として抗菌薬が疑われたため，若干の文献
を加え報告する．

508]
症候群でCV/eGFRは造影剤腎症発症を予測するか
学歯学部附属村上記念病院腎臓内科[1], 朝日大学歯学部附属村
病院泌尿器科[2], 石黒クリニック内科[3]
裕敏（いしがき　ひろとし）[1], 泉久美子[1], 大野道也[1],
司[1], 大橋宏重[1], 江原英俊[2], 石黒源之[3]

糸球体機能（eGFR）に対するヨード造影剤投与量（CV）が，
症候群（ACS）での冠動脈造影（CAG）後の急性腎障害（AKI）
予測するか否か検討した．
ACSでCAGが施行された86名を対象にした．CV/eGFR＜2.0
2.0～3.0をB群，＞3.0をC群とした．AKI発症は造影剤
後に投与前に比較して血清クレアチニン（Cr）0.5mg/dL以上，
25%以上まで上昇するものとした．
CV/eGFRはA群29.5%，B群34.5%，C群36.0%であった．
24名（27.9%）に発症したが，A群に比較してC群で多く認
た．安定狭心症（SAP），不安定狭心症（UAP）ではCV/
が上昇するにつれAKIが発症する傾向を示したが有意でなく，
筋梗塞（AMI）においてのみC群でAKIが多く発症した．
ACSではCAG後に27.8%にAKIが発症した．SAP，UAP
してAMIでCV/eGFR＞3がAKI発症を予測した．

【P-3-509】
血液透析を要した非黄疸性レプトスピラ症の一例
横浜市南部病院腎臓高血圧内科
○北澤篤志（きたざわ　あつし），江原洋介，小川桃子，小野秀二，岩本彩雄

【症例】53歳男性．2013年8月西表島で沢の水を大量摂取．11日後発熱，倦怠感，頭痛，嘔吐，下痢が出現し14日後に帰省．症状改善しないため当院受診し髄膜刺激症状，血小板減少，腎障害，肝障害，炎症反応高値を認めたため入院．髄液検査にて髄膜炎は否定され，経過からレプトスピラ症を疑ったが黄疸は認めず，腸炎症状が主体であった．不明熱として抗菌薬加療を開始したが腎障害，血小板減少は増悪し血圧低下も認めた．横紋筋融解も併発し乏尿となったため第3病日血液透析を併用した．腎機能は次第に軽快し，第10病日退院．入院時の血清PCR検査でレプトスピラ症の確定診断が得られた．
【考察】非黄疸性のレプトスピラ症は従来軽症とされ，また本症例の血清型はWeil病（重症型）とは異なるserovar Grippotyphosaであったにも関わらず透析を要するほどに腎障害は重篤化した．多彩な臨床症状を呈したが筋肉痛，黄疸，ビリルビン上昇など典型的な症状は一切伴わなかったため診断に苦慮した一例であり，若干の文献的考察を加えてここに報告する．

【P-3-510】
急性腎障害を主徴としたレプトスピラ症の一例
東北大学病院
○青木　聡（あおき　さとし），中山恵輔，村田弥栄子，芦野有悟，宮崎真理子，清元秀泰，佐藤　博，伊藤貞嘉

【症例】40歳男性．3週間前タイへ旅行．1週間前より頭痛，発熱が出現．2日前近医脳外科初診．頭部MRI画像，髄液検査所見は異常なし．WBC 8,500/μL，CRP 18.9 mg/dL，Cr 4.8 mg/dLと，炎症反応上昇に加え急性腎障害を呈していたため，精査加療目的に当院紹介・入院．T-Bil 1.6 mg/dL，AST 48 IU/L，ALT 46 IU/Lと軽度肝障害あり．Plt 10.9×10⁴/μLとやや低値も，PT-INR，APTT延長なし．何らかの感染症を考え，CFPM 2 g/日，MINO 100 mg/日投与開始．第2病日，乏尿が続いたため血液透析療法開始．入院初期には腹痛の訴えが目立ったが，炎症反応の低下とともに症状は軽快．尿量漸増し第11病日に透析離脱．ペア血清において抗レプトスピラ抗体の陽転化を認めたため，同症と診断した．
【考察】急性腎障害を主徴としたレプトスピラ症の一例である．本例は重症型と考えられたが，黄疸や出血傾向は目立たなかった．海外渡航歴を有する急性腎障害例では，本疾患を鑑別に挙げることが重要と思われる．

【P-3-511】
抗GBM抗体型急速進行性糸球体腎炎にTTPを合併し，救命し得た一例
呉共済病院腎臓内科
○山田有美（やまだ　ゆみ），森井健一，大久保友恵，青木明日香，平井隆之，久傳康史，藤原謙太，小野哲也

【症例】54歳，女性．
【臨床経過】高血圧症のため近医加療中．入院1か月前より感冒症状が持続し，2週間前より食欲不振，倦怠感も出現した．前医にて検尿異常，高度腎機能障害（UN 161mg/dl，Cr 14.56mg/dl），炎症反応高値を指摘され，当科紹介入院した．尿毒症症状，肺水腫を呈し，同日緊急透析を施行した．抗糸球体基底膜（GBM）抗体定量値は205EUと高値であり，抗GBM抗体型急速進行性糸球体腎炎と診断した．ステロイドパルス療法施行後，プレドニゾロン0.9mg/kg/日の内服に加え血漿交換も併用した．入院時の末梢血中に破砕赤血球がみられ，血小板減少，ADAMTS-13活性の低下より，血栓性血小板減少性紫斑病（TTP）の合併が示唆された．ステロイド治療，血漿交換にて第46病日には抗GBM抗体は陰転化し，外来維持透析へ移行した．TTPに関しては血小板数は正常化し，現在も再燃なく経過している．
【結語】抗GBM抗体型急速進行性糸球体腎炎にTTPを合併した症例は少なく貴重な一例を経験したので報告する．

Tuberculosis 95 (2015) 37–39

Contents lists available at ScienceDirect

Tuberculosis

journal homepage: http://intl.elsevierhealth.com/journals/tube

MOLECULAR ASPECTS

Complete annotated genome sequence of *Mycobacterium tuberculosis* (Zopf) Lehmann and Neumann (ATCC35812) (Kurono)

Tohru Miyoshi-Akiyama [a, d, *], Kazuhito Satou [b], Masako Kato [a], Akino Shiroma [b], Kazunori Matsumura [a], Hinako Tamotsu [b], Hiroki Iwai [a], Kuniko Teruya [b], Keiji Funatogawa [c], Takashi Hirano [b], Teruo Kirikae [a]

[a] *Department of Infectious Diseases, Research Institute, National Center for Global Health and Medicine, 1-21-1 Toyama, Shinjuku, Tokyo, 162-8655, Japan*
[b] *Okinawa Life Science Research Center, 5-8 Suzaki, Uruma, Okinawa, 904-2234, Japan*
[c] *Tochigi Prefectural Institute of Public Health and Environmental Science, 2145-13 Shimookamoto, Kawachi-machi, Tochigi, 329-1196, Japan*
[d] *Pathogenic Microbe Laboratory, Research Institute, National Center for Global Health and Medicine, 1-21-1 Toyama, Shinjuku, Tokyo, 162-8655, Japan*

ARTICLE INFO

Article history:
Received 14 April 2014
Received in revised form
8 August 2014
Accepted 19 October 2014

Keywords:
PacBio sequencer
Kurono
PE-PPE
Phyrogenetic tree
Complete genome

SUMMARY

We report the completely annotated genome sequence of Mycobacterium tuberculosis (Zopf) Lehmann and Neumann (ATCC35812) (Kurono), which is a used for virulence and/or immunization studies. The complete genome sequence of M. tuberculosis Kurono was determined with a length of 4,415,078 bp and a G+C content of 65.60%. The chromosome was shown to contain a total of 4,340 protein-coding genes, 53 tRNA genes, one transfer messenger RNA for all amino acids, and 1 rrn operon. Lineage analysis based on large sequence polymorphisms indicated that M. tuberculosis Kurono belongs to the Euro-American lineage (lineage 4). Phylogenetic analysis using whole genome sequences of M. tuberculosis Kurono in addition to 22 M. tuberculosis complex strains indicated that H37Rv is the closest relative of Kurono based on the results of phylogenetic analysis. These findings provide a basis for research using M. tuberculosis Kurono, especially in animal models.

We report the completely annotated genome sequence of *Mycobacterium tuberculosis* (Zopf) Lehmann and Neumann (ATCC35812) (Kurono), which is a used for virulence and/or immunization studies primarily in Japan.

M. tuberculosis strain Kurono was isolated from human sputum by Mizunoe in 1951 at Kitasato Research Institute, Tokyo, Japan, and deposited with the Trudeau Mycobacterium Culture Collection in 1969 [1]. Due to its consistently moderate virulence, it has been widely used as a standard virulent laboratory strain for virulence and immunization studies primarily in Japan.

Genome sequence data of *M. tuberculosis* Kurono were obtained using Pacific Biosciences' Single-Molecule Real Time (SMRT) sequencing technology [2] according to the Greater Than 10 kb Template Preparation and Sequencing protocol provided by Pacific Biosciences (Menlo Park, CA). The libraries were prepared, and sequencing was conducted according to the manufacturer's protocols. Briefly, the extracted DNA was purified using a PowerClean DNA Clean-Up Kit (MoBio laboratories, Carlsbad, CA) and concentrated using AMPure XP (Beckman Coulter, Brea, CA) of 0.45x. SMRTbell 20 kb libraries were prepared using the 3 kb–10 kb Template Prep Kit 2.0 (Pacific Biosciences). Libraries were subsequently sequenced on the PacBio RS II sequencing platform (Pacific Biosciences) using DNA/Polymerase Binding Kit P4 (Pacific Biosciences) and DNA Sequencing Kit 2.0 (Pacific Biosciences). Titration density was 0.0169 nM. Template was loaded into SMRT Cell 3.0 (Pacific Biosciences) using a Mag Bead Kit (Pacific Biosciences). Sequencing was performed using 16 cells. A movie of 120 min was taken for each cell.

The complete genome sequence of *M. tuberculosis* Kurono was determined using the Hierarchical Genome Assembly Process (HGAP) [3]. We used version 2 of the HGAP workflow implemented in version 2.1.1 of SMRT Analysis (Pacific Biosciences), a powerful, open-source bioinformatics software suite available for analysis of DNA sequencing data from PacBio SMRT technology. HGAP consists of preassembly, assembly with Celera Assembler [4], and consensus polishing with Quiver [3]. After default quality filtering, 1,988,205 reads were obtained with a mean length of 2240 bp totaling 4,455,125,637 bp. The preassembly process with a length cutoff of 8,875 bp generated 14,126 long and error-corrected reads with a

* Corresponding author. Department of Infectious Diseases, Research Institute, National Center for Global Health and Medicine, 1-21-1 Toyama, Shinjuku-ku, Tokyo 162-8655, Japan. Tel.: +81 3 3202 7181x2903; fax: +81 3 3202 7364.
E-mail address: takiyam@ri.ncgm.go.jp (T. Miyoshi-Akiyama).

http://dx.doi.org/10.1016/j.tube.2014.10.007
1472-9792/

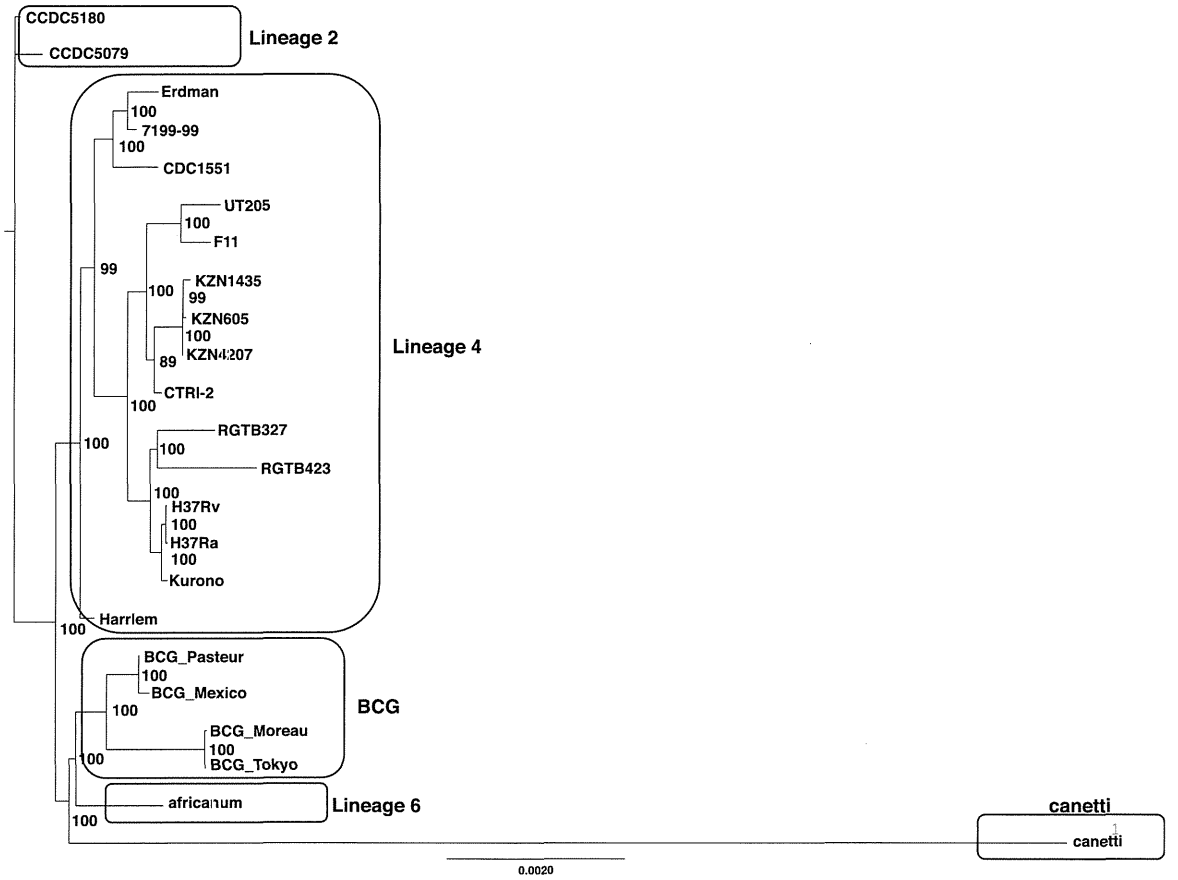

Figure 1. Maximum-likelihood phylogenies based on whole genome sequence alignment of *M. tuberculosis* complex. Phylogenetic trees based on whole genome sequences of *M. tuberculosis* complex were constructed using PhyML 3.0. One hundred bootstrap re-samplings were performed for each tree. KZN series strains harbor large inversion in their genome. Thus, inversion-corrected sequences were used for the alignment and marked "_m". Accession numbers of each sequence used was following: CCDC5079: CP001642.1; CCDC5180: CP001642.1; CDC1551: AE000516.2; CTRI-2: CP002992.1; Erdman: AP012340.1; F11: CP000717.1; H37Ra: CP000611.1.; H37Rv: AL123456.2; KZN605: CP001976.1; KZN1435: CP001658.1; KZN4207: CP001662.1; RGTB327: CP003233.1; RGTB423: CP003234.1; Mexico: CP002095.1; Moreau RDJ: AM412059.2; Pasteur: AM408590.1; Tokyo 172: AP010918.1; GMO41182: FR878060.1; CIPT 140010059: HE572590.1.

mean length of 5732 bp totaling 80,976,246 bp. Subsequently, the assembly process constructed a single contig with a length of 4,423,481 bp. Finally, the consensus polishing process output a highly accurate self-overlapping contig with a length of 4,424,104 bp. After circularizing and trimming, the complete genome sequence of *M. tuberculosis* Kurono was determined with a length of 4,415,078 bp and a G + C content of 65.60%.

Primary coding sequence extraction was performed by glimmer (http://www.ncbi.nlm.nih.gov/genomes/MICROBES/glimmer_3.cgi). The results were compared to verify the annotation, and were corrected manually by *in silico* molecular cloning (in Silico Biology Inc., Kanagawa, Japan). The chromosome was shown to contain a total of 4340 protein-coding genes, 53 tRNA genes, one transfer messenger RNA for all amino acids, and 1 *rrn* operon. In addition, the chromosome harbors 14 IS6110 sequences. There is no known mutation related to drug resistance in the genome. Nucleotide sequences of the chromosome of *M. tuberculosis* Kurono have been deposited in the DNA Database of Japan under accession no. AP014573.

Lineage analysis based on large sequence polymorphisms (LSP) [5] indicated that *M. tuberculosis* Kurono belongs to the Euro-American lineage (lineage 4). Phylogenetic analysis using whole genome sequences of *M. tuberculosis* Kurono in addition to 22 *M. tuberculosis* complex strains available by April 2012 were performed after exclusion of regions encoding PE/PPE families using R (http://www.r-project.org) with a package, Biostrings (http://www.bioconductor.org/packages/release/bioc/html/Biostrings.html) because of their homoplastic nature. Genome sequence alignment was prepared using MAFFT software version 7 (http://mafft.cbrc.jp/alignment/server/). PE/PPE regions excluded from the analysis and resulted alignments are available by request. Based on the alignment, three phylogenetic methods were used to evaluate robustness of the trees: a maximum-likelihood approach (PhyML 3.0 http://www.atgc-montpellier.fr/phyml/). HYK and gamma were chosen for a nucleotide substitution model, and tree robustness was evaluated by aLRT. The resulting phylogenies were largely congruent. Each clade consisted of a particular LSP lineage. The clade containing *M. tuberculosis* Kurono included four other lineage strains, such as H37Rv. H37Rv is the closest relative of Kurono based on the results of phylogenetic analysis. There were only 818 SNPs between H37Rv and Kurono, and almost 40% of the SNPs are located in the PE-PPE family proteins. These findings provide a basis for research using *M. tuberculosis* Kurono, especially in animal models. Figure 1.

Acknowledgments

T. K. and T. M. A. were supported by Grants for International Health Research (24A-103) and (26A-103) from the Ministry of Health, Labor, and Welfare of Japan, respectively. The funding

resources did not have any roles in this study. The authors thank Mrs. Komiya and Mrs. Sakurai for their excellent work in the genome analysis.

Funding: None.

Competing interest: None to declare.

Ethical approval: Not required.

References

[1] Trudeau Institute. In: Trudeau mycobacterial culture collection, U.S.–Japan cooperative medical science program, geographic medical branch, National Institute of Allergy and Infectious Diseases, National Institutes of Health, Bethesda, Maryland; 1972. TMC #124, p. 24.

[2] Eid J, Fehr A, Gray J, Luong K, Lyle J, Otto G, Peluso P, Rank D, Baybayan P, Bettman B, Bibillo A, Bjornson K, Chaudhuri B, Christians F, Cicero R, Clark S, Dalal R, Dewinter A, Dixon J, Foquet M, Gaertner A, Hardenbol P, Heiner C, Hester K, Holden D, Kearns G, Kong X, Kuse R, Lacroix Y, Lin S, Lundquist P, Ma C, Marks P, Maxham M, Murphy D, Park I, Pham T, Phillips M, Roy J, Sebra R, Shen G, Sorenson J, Tomaney A, Travers K, Trulson M, Vieceli J, Wegener J, Wu D, Yang A, Zaccarin D, Zhao P, Zhong F, Korlach J, Turner S. Real-time DNA sequencing from single polymerase molecules. Science 2009;323(5910):133–8.

[3] Chin CS, Alexander DH, Marks P, Klammer AA, Drake J, Heiner C, Clum A, Copeland A, Huddleston J, Eichler EE, Turner SW, Korlach J. Nonhybrid, finished microbial genome assemblies from long-read SMRT sequencing data. Nat Methods 2013;10(6):563–9.

[4] Myers EW, Sutton GG, Delcher AL, Dew IM, Fasulo DP, Flanigan MJ, Kravitz SA, Mobarry CM, Reinert KH, Remington KA, Anson EL, Bolanos RA, Chou HH, Jordan CM, Halpern AL, Lonardi S, Beasley EM, Brandon RC, Chen L, Dunn PJ, Lai Z, Liang Y, Nusskern DR, Zhan M, Zhang Q, Zheng X, Rubin GM, Adams MD, Venter JC. A whole-genome assembly of *Drosophila*. Science 2000;287(5461):2196–204.

[5] Hirsh AE, Tsolaki AG, DeRiemer K, Feldman MW, Small PM. Stable association between strains of *Mycobacterium tuberculosis* and their human host populations. Proc Natl Acad Sci U S A 2004;101(14):4871–6.

Molecular Microbiology (2014) 91(3), 538–547

doi:10.1111/mmi.12476
First published online 9 January 2014

A silent mutation in *mabA* confers isoniazid resistance on *Mycobacterium tuberculosis*

Hiroki Ando,† Tohru Miyoshi-Akiyama, Shinya Watanabe and Teruo Kirikae*
Department of Infectious Diseases, Research Institute, National Center for Global Health and Medicine, 1-21-1 Toyama, Shinjuku, Tokyo 162-8655, Japan.

Summary

Drug resistance in *Mycobacterium tuberculosis* (*Mtb*) is caused by mutations in restricted regions of the genome. Mutations in *katG*, the promoter region of the *mabA–inhA* operon, and *inhA* are those most frequently responsible for isoniazid (INH) resistance. Several INH-resistant (INH^r) *Mtb* clinical isolates without mutations in these regions have been described, however, indicating that there are as yet undetermined mechanisms of INH resistance. We identified the *mabA*^{g609a} silent mutation in a significant number of INH^r *Mtb* clinical isolates without known INH resistance mutations. A laboratory strain, H37Rv, constructed with *mabA*^{g609a}, was resistant to INH. We show here that the *mabA*^{g609a} mutation resulted in the upregulation of *inhA*, a gene encoding a target for INH, converting the region adjacent to the mutation into an alternative promoter for *inhA*. The *mabA*^{g609a} silent mutation results in a novel mechanism of INH resistance, filling in a missing piece of INH resistance in *Mtb*.

Introduction

Tuberculosis (TB) remains a challenging disease throughout the world. For example, in 2012 there were 8.6 million incident cases of TB and 1.3 million deaths from this disease among HIV-negative people, and an additional 0.3 million deaths from HIV-associated TB (World Health Organization, 2013).

Isoniazid (INH) is the most widely used and one of the most effective first-line anti-TB drugs in current use, being a keystone of treatment since its introduction in 1952 (Bernstein *et al.*, 1952). However, the emergence of INH-resistant (INH^r) *Mycobacterium tuberculosis* (*Mtb*) is a serious threat to the control of TB (Espinal *et al.*, 2001). There is considerable interest in identifying the molecular basis of INH resistance in clinical *Mtb* isolates, both to develop rapid diagnostic assays to detect INH^r *Mtb* strains and to develop novel anti-TB drugs.

INH is a prodrug that is activated by the bifunctional catalase-peroxidase enzyme KatG, encoded by the *katG* gene (Zhang *et al.*, 1992). Activated INH blocks the synthesis of essential mycolic acids by inhibiting the NADH-dependent enoyl-acyl carrier protein reductase InhA (Banerjee *et al.*, 1994; Vilcheze *et al.*, 2006). INH^r clinical isolates often lose the catalase and peroxidase activities of KatG, resulting in high-level INH resistance (Zhang and Yew, 2009; Ando *et al.*, 2010). The KatG^{S315T} mutation is the most common mutation in INH^r strains (Hazbon *et al.*, 2006; Zhang and Yew, 2009). INH resistance is also conferred by mutations in the promoter region of the *mabA–inhA* operon, causing overexpression of InhA, or by mutations at the InhA active site, lowering InhA affinity to activated INH (Banerjee *et al.*, 1994; Rozwarski *et al.*, 1998; Vilcheze *et al.*, 2006; Zhang and Yew, 2009). These mutations also confer resistance to the INH-related drug ethionamide (ETH) (Banerjee *et al.*, 1994; Vilcheze *et al.*, 2006). Mutations in the promoter region of the *mabA–inhA* operon or in *inhA* are usually associated with low-level resistance and are less frequent than mutations in *katG* (Hazbon *et al.*, 2006; Zhang and Yew, 2009). Thus, mutations in *katG*, the promoter region of the *mabA–inhA* operon, and *inhA* are those most frequently responsible for INH resistance. However, mutations in these regions are absent from 10–25% of INH^r *Mtb* clinical isolates (Ramaswamy and Musser, 1998; Ramaswamy *et al.*, 2003; 2004; Zhang *et al.*, 2005; Hazbon *et al.*, 2006; Zhang and Yew, 2009), consistent with our previous report showing that 23% of INH^r *Mtb* isolates had no mutation (Ando *et al.*, 2010). Taken together, these findings indicate that a significant numbers of INH^r *Mtb* clinical isolates are resistant to INH through as yet undetermined mechanisms.

We reported that 19% (20 of 108) of INH^r isolates had the *mabA*^{g609a} silent mutation (Ando *et al.*, 2010); of these 20 isolates, 17 had no additional mutations in the *furA–katG* and *mabA–inhA* operons and in –200bp of the promoter region of the *mabA–inhA* operon (Ando *et al.*,

Accepted 29 November, 2013. *For correspondence. E-mail tkirikae@ri.ncgm.go.jp; Tel. (+81) 3 3202 7181, ext. 2838; Fax (+81) 3 3202 7364. †Present address: Department of Electrical Engineering & Computer Science and Department of Biological Engineering, Massachusetts Institute of Technology, Cambridge, MA 02139, USA.

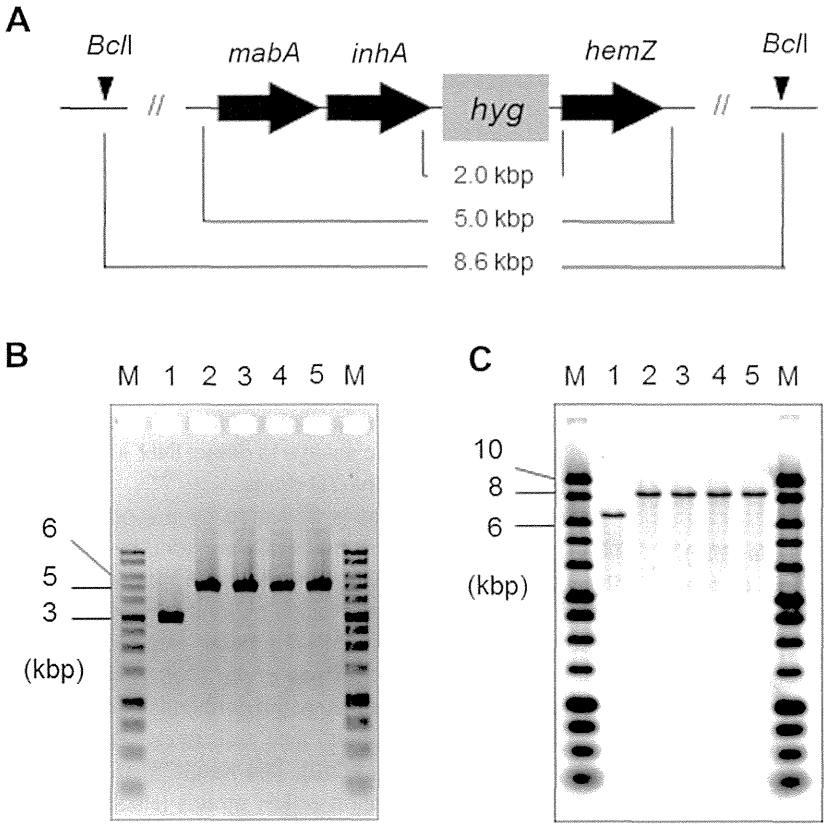

Fig. 1. Construction of the H37Rv isogenic strains. (A) Schematic representation of the H37Rv isogenic strain. These strains were confirmed as having the correct chromosomal structures by (B) PCR using locus-specific primers and by (C) Southern blotting using an HRP-labelled *mabA–inhA* probe. M, size marker; 1, H37Rv; 2, $mabA^{WT}$ strain #1; 3, $mabA^{WT}$ strain #2; 4, $mabA^{g609a}$ strain #1; 5, $mabA^{g609a}$ strain #2.

2010). A comprehensive multicenter study also found this mutation in 14% (20 of 138) of INH^r isolates, with 17 of the 20 isolates having no other INH^r mutations (Mitarai *et al.*, 2012). A synonymous substitution in MabA codon 203, corresponding to nucleotide 607–609 in *mabA*, was reported in an INH^r *Mtb* clinical isolate (Ramaswamy *et al.*, 2003). Moreover, to date, and including our unpublished results, 410 INH-susceptible (INH^s) isolates tested did not have the $mabA^{g609a}$ mutation, and, to our knowledge, this mutation has never been detected in INH^s isolates, suggesting that this mutation may be associated with INH resistance in *Mtb*. In contrast MabA was reported to be unrelated to INH resistance, since its overexpression fails to confer resistance to INH (Banerjee *et al.*, 1998). Based on these findings, we investigated the role of the $mabA^{g609a}$ silent mutation in the INH resistance of *Mtb*.

We describe here a novel mechanism of INH resistance in *Mtb*. The $mabA^{g609a}$ silent mutation confers INH resistance on *Mtb* by increasing the transcriptional levels of *inhA*. The $mabA^{g609a}$ mutation and its adjacent region act as a promoter for the expression of *inhA*. Considerable numbers of INH^r clinical isolates have this mutation (Ando *et al.*, 2010; Mitarai *et al.*, 2012). The $mabA^{g609a}$ silent mutation yields important insight into INH resistance in *Mtb*.

Results

Reconstruction of $mabA^{g609a}$ in a laboratory strain H37Rv

To examine whether $mabA^{g609a}$ confers resistance to INH on a clean genetic background, we performed a specialized transduction to introduce this mutation, linked to a gene conferring resistance to hygromycin, into the *Mtb* laboratory strain H37Rv (Fig. 1A). Two types of hygromycin-resistant transductants were generated, differing in their sites of recombination with respect to the g609a mutation, and yielding isogenic strains, $mabA^{g609a}$ and $mabA^{WT}$. The correct chromosomal structures of these strains were confirmed by PCR amplification (Fig. 1B), Southern blotting (Fig. 1C), and sequencing (see *Experimental procedures*).

$mabA^{g609a}$ confers resistance to INH and ETH

The $mabA^{g609a}$ strains showed resistance to INH, with MICs of 0.5 μg ml^{-1}, whereas the MICs of $mabA^{WT}$ were 0.1 μg ml^{-1}, equal to that of the parental H37Rv strain (Table 1). We also determined the MICs of these strains to ETH, because INH^r strains carrying a mutation in the *mabA–inhA* operon showed resistance to ETH due to overexpression of *inhA* or reduced InhA affinity to ETH

Table 1. The MICs for INH and ETH.

Strain	Description	MIC (mg ml^{-1}) INH	ETH
H37Rv	Laboratory strain, wild-type	0.1	2
mabA^{WT} #1	H37Rv *mabA–inhA-hyg*	0.1	1
mabA^{WT} #2	H37Rv *mabA–inhA-hyg*	0.1	2
mabA^{g609a} #1	H37Rv *mabA*^{g609a}*–inhA-hyg*	0.5	16
mabA^{g609a} #2	H37Rv *mabA*^{g609a}*–inhA-hyg*	0.5	16
NCGM2840	Clinical isolate, *mabA*^{g609a}	0.4	16
NCGM2854	Clinical isolate, *mabA*^{g609a}	0.3	32
NCGM2860	Clinical isolate, *mabA*^{g609a}	0.4	32
NCGM2872	Clinical isolate, *mabA*^{g609a}	0.4	64
NCGM2933	Clinical isolate, *mabA*^{g609a}	0.3	16
NCGM2943	Clinical isolate, *mabA*^{g609a}	0.4	32

(Vilcheze *et al.*, 2006). The *mabA*^{g609a} strains showed resistance to ETH, with MICs of 16 μg ml^{-1}, whereas the MICs of *mabA*^{WT} and the H37Rv were 2.0 μg ml^{-1} (Table 1). Furthermore, INH^r clinical isolates carrying the *mabA*^{g609a} genes (NCGM2840, 2854, 2860, 2872, 2933 and 2943) showed resistance to both INH and ETH (Table 1). These strains had no other mutation in the *furA–katG* and *mabA–inhA* operons and in their promoter regions. These results clearly indicate that the *mabA*^{g609a} silent mutation confers resistance to both INH and ETH on *Mtb*.

mabA^{g609a} *upregulates the transcriptional levels of inhA*

Because resistance to INH is mediated by the overexpression of *inhA* (Larsen *et al.*, 2002) and/or the downregulation of *katG* (Ando *et al.*, 2011), we compared the levels of InhA and KatG proteins in *mabA*^{g609a} and *mabA*^{WT} by Western blotting. We found that the levels of InhA were significantly greater in *mabA*^{g609a} (Fig. 2A, left panel lanes 4, 5) than in *mabA*^{WT} (Fig. 2A, left panel lanes 1–3), whereas the levels of KatG and HSP70, an internal control (Fig. 2A, right panel), were similar. Using qRT-PCR, we assessed whether the increased expression of *inhA* in *mabA*^{g609a} resulted from increased transcription or post-transcriptional activation. The levels of *inhA* mRNA were significantly higher in *mabA*^{g609a} than in *mabA*^{WT}

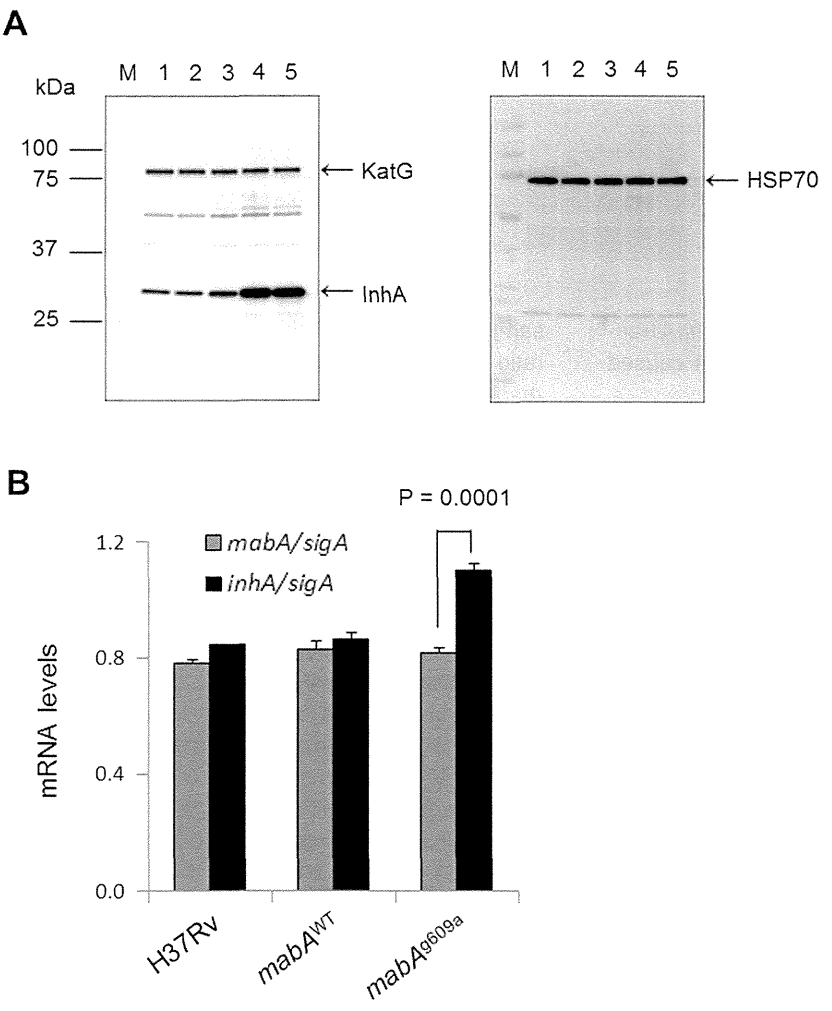

Fig. 2. *mabA*^{g609a} upregulates *inhA* expression.
A. Western blotting analysis of InhA, KatG and HSP70 proteins in the isogenic strains. M, size marker; 1, H37Rv; 2, *mabA*^{WT} strain #1; 3, *mabA*^{WT} strain #2; 4, *mabA*^{g609a} strain #1; 5, *mabA*^{g609a} strain #2.
B. qRT-PCR analysis of *mabA* and *inhA* mRNA in the isogenic strains. Levels of *mabA* and *inhA* mRNA were normalized relative to those of *sigA* mRNA. Means ($n = 3$) ± SD.

Table 2. Levels of expression of *mabA* and *inhA* by RNA-seq.

Strain	Description	Gene	Fold-change compared with H37Rv	*inhA*/*mabA* ratio
H37Rv	Laboratory strain, wild-type	*mabA*	1.00	1.00
		inhA	1.00	
mabA^{WT} #1	H37Rv *mabA–inhA-hyg*	*mabA*	0.84	1.46
		inhA	1.23	
mabA^{WT} #2	H37Rv *mabA–inhA-hyg*	*mabA*	0.83	1.24
		inhA	1.03	
mabA^{g609a} #1	H37Rv *mabA*^{g609a}*–inhA-hyg*	*mabA*	0.77	5.52
		inhA	4.25	
mabA^{g609a} #2	H37Rv *mabA*^{g609a}*–inhA-hyg*	*mabA*	0.87	3.62
		inhA	3.15	
NCGM2787	Clinical isolate, wild-type	*mabA*	2.65	1.08
		inhA	2.86	
NCGM2817	Clinical isolate, wild-type	*mabA*	1.57	0.90
		inhA	1.41	
NCGM2840	Clinical isolate, *mabA*^{g609a}	*mabA*	1.12	5.09
		inhA	5.70	
NCGM2854	Clinical isolate, *mabA*^{g609a}	*mabA*	1.58	3.42
		inhA	5.41	
NCGM2860	Clinical isolate, *mabA*^{g609a}	*mabA*	1.11	4.05
		inhA	4.49	
NCGM2872	Clinical isolate, *mabA*^{g609a}	*mabA*	1.47	6.63
		inhA	9.74	
NCGM2933	Clinical isolate, *mabA*^{g609a}	*mabA*	1.03	3.36
		inhA	3.46	
NCGM2943	Clinical isolate, *mabA*^{g609a}	*mabA*	0.90	3.44
		inhA	3.10	
NCGM2791	Clinical isolate, c-15t in the promoter	*mabA*	30.77	0.84
		inhA	25.88	
NCGM2845	Clinical isolate, c-15t in the promoter	*mabA*	35.74	0.68
		inhA	24.28	

Levels of expression of *mabA* and *inhA* were analysed by RNA-seq and normalized to the entire transcriptome. The fold-change of the expression levels were calculated by Kal's test (Kal *et al.*, 1999).

(Fig. 2B), indicating that the mutation enhanced *inhA* transcription and that increased expression of *inhA* caused resistance to INH in *mabA*^{g609a} strains.

mabA^{g609a} *contains additional transcripts of inhA*

To confirm that *inhA* transcription was enhanced in *mabA*^{g609a} strains, we performed RNA-seq on RNAs isolated from H37Rv, isogenic strains (*mabA*^{g609a} #1 and #2, and *mabA*^{WT} #1 and #2), and clinical isolates with (NCGM2840, 2854, 2860, 2872, 2933 and 2943) and without (NCGM2787 and 2817) the *mabA* ^{g609a} mutation (Table 2). More than two million 151 or 251 bp paired-end sequence fragments ('reads') were recovered from each sample and mapped to the H37Rv reference genome. To compare estimated normalized levels of expression of *mabA* and *inhA* in these samples, we calculated reads per kilobase per million mapped reads (RPKM) (Mortazavi *et al.*, 2008), fold-changes in RPKM in these samples compared with H37Rv (Kal *et al.*, 1999), and the ratio of *inhA* to *mabA* expression (Fig. 3A and Table 2). Although the level of *mabA* expression was similar among the samples, the level of *inhA* expression and the *inhA/mabA* ratio were 4.25- and 5.52-fold higher, respectively, in *mabA*^{g609a} #1, and 3.15- and 3.62-fold higher, respectively, in *mabA*^{g609a} #2, than in H37Rv. We observed similar results in the clinical isolates with the *mabA*^{g609a} mutation, with the *inhA*/*mabA* ratio ranging from 3.36 to 6.63. Furthermore, to compare the level of *inhA* expression in these strains with that in a strain bearing the c-15t mutation in the promoter region of the *mabA–inhA* operon, which causes overexpression of *inhA*, we performed RNA-seq on RNAs isolated from clinical isolates with the c-15t mutation (NCGM2791 and 2845). As expected, the expression of both *mabA* and *inhA* was increased in these isolates, with the levels of *inhA* expression higher than in the *mabA*^{g609a} strains (Table 2). These results, and previous findings showing that the c-15t mutation confers a low level of INH resistance on clinical isolates (Ando *et al.*, 2010) and on the H37Rv isogenic strain (Vilcheze *et al.*, 2006), suggest that the increased expression of *inhA* due to the *mabA*^{g609a} mutation was sufficient to confer a low level of INH resistance on these strains, although this level, and even the higher level of expression resulting

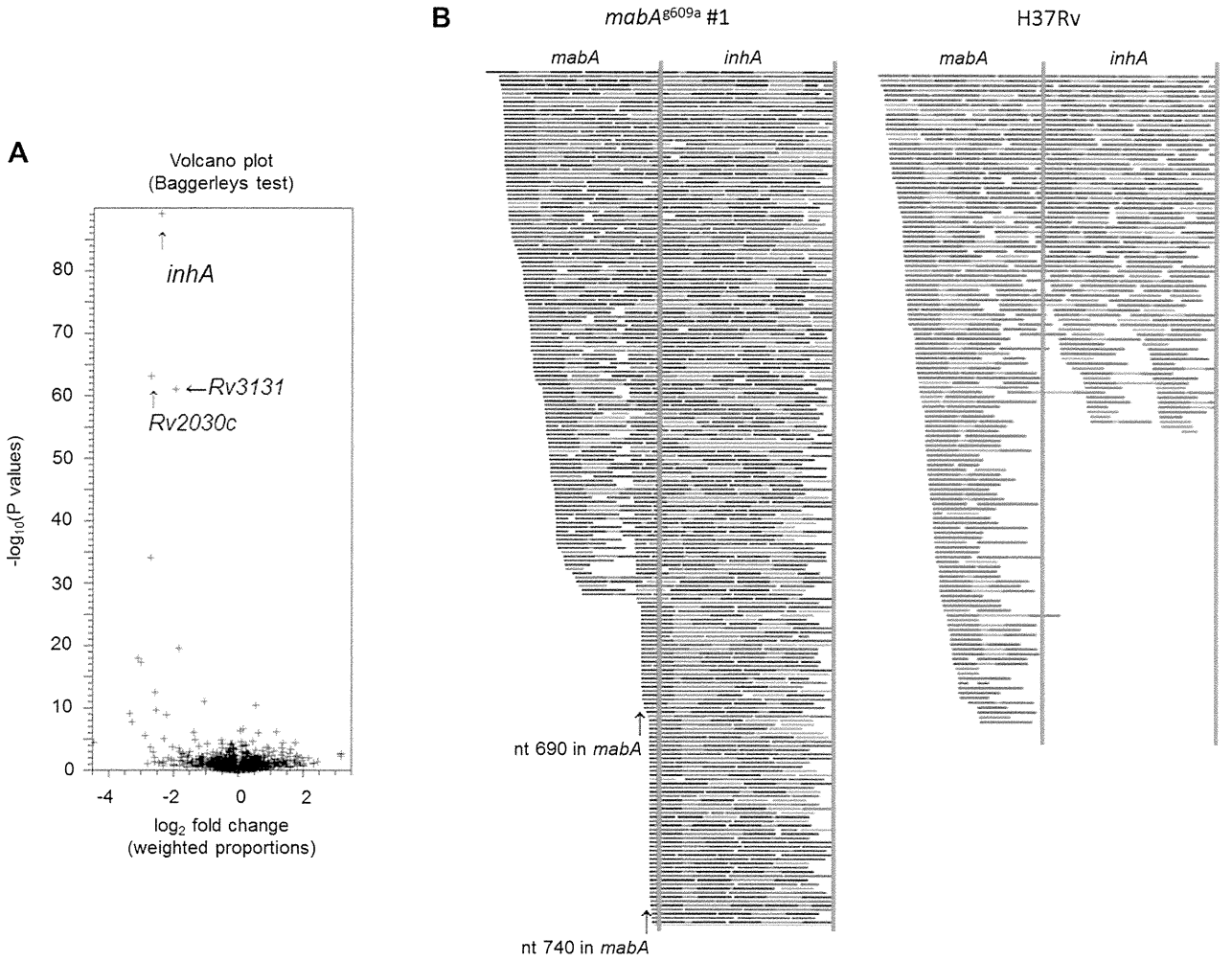

Fig. 3. Impact of *mabA*^{g609a} on *inhA* expression in H37Rv. Whole RNA was sequenced using a MiSeq system, with RNA-seq data visualized on a CLC genomics workbench.
A. Volcano plot (Cui and Churchill, 2003) to identify genes differentially expressed in *mabA*^{WT} and *mabA*^{g609a} strains.
B. Read mapping results in the *mabA–inhA* region of the *mabA*^{g609a} #1 and H37Rv. Red lines indicate the corresponding gene regions for *mabA* and *inhA*. Reads shown in blue are paired-end reads while reads shown in other colours are single reads. Arrows indicate the two dominant transcripts.

from the c-15t mutation in the promoter region of the *mabA–inhA* operon, were insufficient to confer on these strains a high level (1.0 μg ml^{-1}) of INH resistance.

We observed two additional transcripts of *inhA* in the *mabA*^{g609a} strain, starting from nucleotides 690 and 740 in *mabA* (Fig. 3B). This finding suggests that the *mabA*^{g609a} mutation may act as an enhancer of *inhA* transcription, resulting in InhA overexpression and INH resistance.

The region adjacent to the mabA^{g609a} mutation acts as a promoter for inhA

A C-15T mutation in the region upstream of the *mabA–inhA* operon was shown to enhance *inhA* transcription in *Mtb* (Vilcheze *et al.*, 2006), with *cis*-elements, including a promoter region upstream of the *mabA–inhA* operon, required for the (over)expression of *inhA* (Banerjee *et al.*, 1994; Vilcheze *et al.*, 2006). In contrast, the regions upstream of clinical isolates harbouring the *mabA*^{g609a} mutation were not affected by any mutation. These findings and the identification of two additional transcripts of *inhA* (Fig. 3B) allowed us to define the –10 and –35 nucleotide regions of a novel *inhA* promoter generated by the g609a mutation (Fig. 4A). Using the promoter prediction program of GENETYX-MAC (version 16.0.4, Genetyx Corporation), we observed a promoter region in *mabA* carrying the mutation, whereas no such promoter region was observed in H37Rv (Fig. 4A). To confirm that this mutation and its adjacent sequences act as a novel promoter of *inhA* expression, a reporter assay using the pJEM13 (Timm

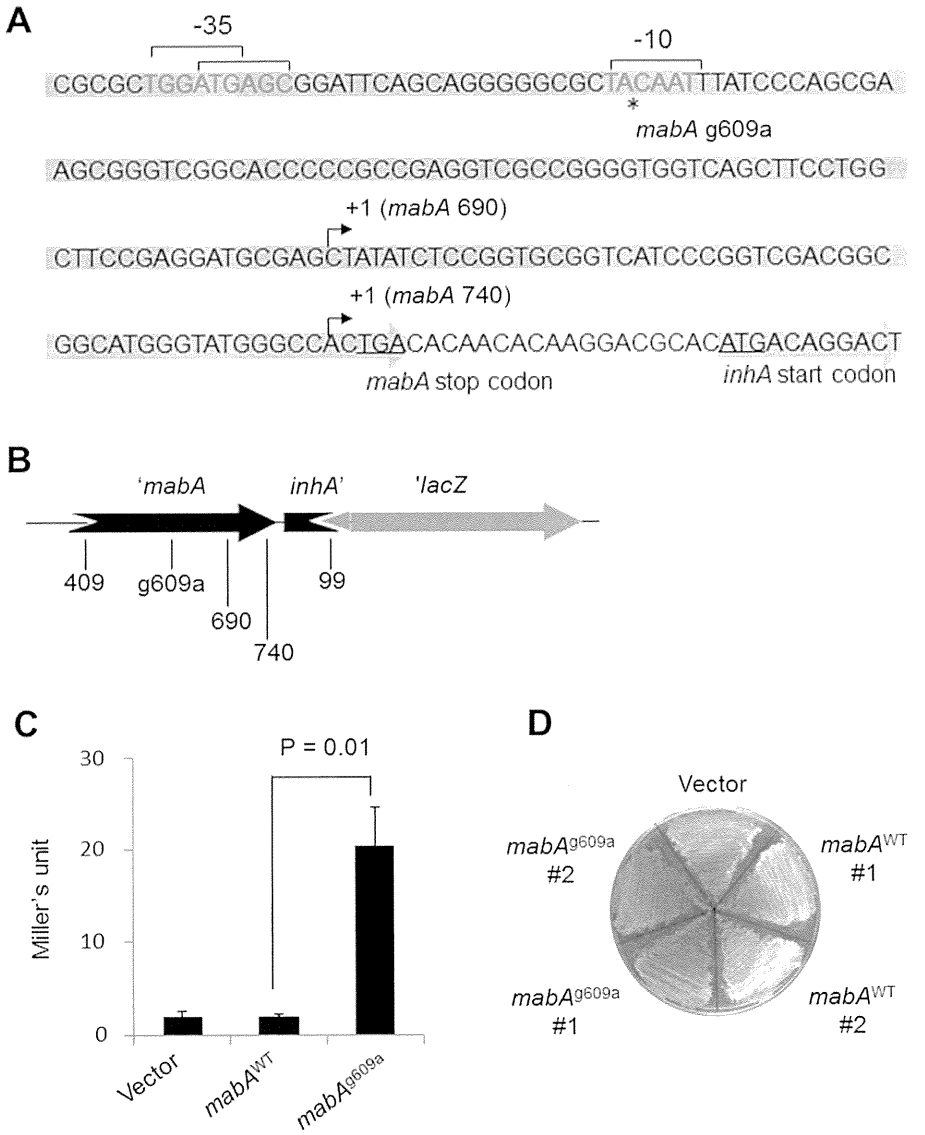

Fig. 4. *mabA*^{g609a} and its adjacent region acts as a promoter for *inhA*.
A. Predicted –10 and –35 regions of an additional *inhA* promoter. The –10 and –35 regions are indicated in red. The *mabA*^{g609a} mutation is noted with an asterisk. The transcription start sites are denoted by bent arrows. ORFs are shaded in blue and the *mabA* stop and *inhA* start codons are underlined.
B. Schematic representation of pJEM13–*mabA*^{g609a}–*inhA*–*lacZ* fusion without the native promoter region of the *mabA*–*inhA* operon. The fusion contains the region from nucleotide 409 of *mabA* to nucleotide 99 of *inhA*. The *mabA*^{g609a} mutation and the transcription start sites (690 and 740) are indicated.
C. β-Galactosidase assay of H37Rv transformant with pJEM13-derived fusion. β-galactosidase activity was calculated in Miller's units. Means ($n = 3$) ± SD.
D. β-Galactosidase activity was monitored by streaking transformants onto 7H10-OADC plates containing X-Gal.

et al., 1994) vector was used to measure the effect of *mabA*^{g609a} on *inhA* expression in *Mtb* H37Rv. Use of the pJEM13–*mabA*^{g609a}–*inhA*–*lacZ* fusion plasmid, which lacks the native promoter region of the *mabA*–*inhA* operon (Fig. 4B), showed that *mabA*^{g609a} significantly enhanced *inhA*–*lacZ* expression (Fig. 4C and D), whereas *mabA* without the mutation did not, when compared with vector controls. These results, in addition to the RNA-seq analysis, clearly indicate that a region adjacent to the g609a mutation in *mabA* acts as a promoter of *inhA* expression.

Discussion

We have shown here that the *mabA*^{g609a} silent mutation confers resistance to INH and ETH on *Mtb*. This is a novel and alternative mechanism of *inhA* overexpression. A labo-

ratory strain H37Rv containing this mutation expressed significantly higher amounts of InhA, due to increased levels of *inhA* transcripts, and was resistant to INH. The *mabA*^{g609a} mutation and the region adjacent to it act as an *inhA* promoter. The *mabA*^{g609a} mutation may also affect levels of *inhA* transcripts by increasing the stability of these transcripts and by altering an RNase cleavage site in *mabA–inhA* mRNA. *Mtb* carrying this mutation acquires resistance to INH without reducing the fitness of MabA mutants, since this mutation is silent and *mabA* is an essential gene.

Although the major causes of INH resistance are mutation(s) in *katG* and/or the promoter region of the *mabA–inhA* operon, these mutations are absent from a significant percentage of INH^r clinical isolates. To our knowledge, five reports have described INH-resistance-related genes or regions with isogenic *Mtb* strains, in addition to mutations in the *katG* region and the promoter region of the *mabA–inhA* operon (Buchmeier *et al.*, 2003; Vilcheze *et al.*, 2006; 2008; Ando *et al.*, 2011; Lee *et al.*, 2012). An InhA^{S94A} mutation at the active site resulted in reduced InhA affinity to activated INH, resulting in resistance to INH (Vilcheze *et al.*, 2006). In addition, *sigI*, which encodes sigma factor I, has been associated with INH resistance in *Mtb*, with SigI-mediated downregulation of *katG* expression conferring resistance to INH (Lee *et al.*, 2012). To date, however, clinical isolates with *sigI* mutations have not been identified. Deletion of *mshA*, which encodes a glycosyltransferase involved in mycothiol biosynthesis, from the H37Rv, CDC1551, and Erdman strains, found that only the CDC1551 Δ*mshA* strain showed increased MIC to INH. Moreover, disruption of *mshB*, which encodes a deacetylase involved in mycothiol biosynthesis, resulted in a twofold increase in MIC to INH. We recently reported that mutations in the intergenic region of the *furA–katG* operon downregulated *katG* expression and conferred resistance to INH; and that the c41t mutation in *furA*, which encodes a negative regulator of the *furA–katG* operon, resulted in a twofold increase in MIC of INH (Ando *et al.*, 2011). It is still unclear whether the *mshA* and *mshB* genes and the *furA*^{c41t} mutation are associated with resistance to INH, because their MICs to INH increased only twofold. Several genes have been reported as candidate genes for INH resistance, including *kasA*, *dfrA*, *ahpC*, *ndh* and *mshC*. In contrast, *kasA*, *dfrA* and *ahpC* were unrelated to INH resistance in *Mtb* (Heym *et al.*, 1997; Larsen *et al.*, 2002; Wang *et al.*, 2010). The *ndh* and *mshC* genes were shown related to INH resistance in *Mycobacterium smegmatis* and/or *Mycobacterium bovis* BCG but not in *Mtb* (Vilcheze *et al.*, 2005; 2011). Although mutations in the intergenic region of the *furA–katG* operon (Ando *et al.*, 2011) and the InhA^{S94A} mutation (Vilcheze *et al.*, 2006) have been observed in INH^r clinical isolates, these are rare and cannot fully explain the INH resistance mechanisms of isolates without mutations in *katG* and the promoter region of the *mabA–inhA* operon.

The *mabA*^{g609a} mutation was not laboratory-selected; rather, it has been observed in a significant proportion of INH^r clinical isolates (Ando *et al.*, 2010; Mitarai *et al.*, 2012). To our knowledge, this report is the first to show that this silent mutation confers resistance to antibiotics, including INH and ETH. The role of the *mabA*^{g609a} mutation in *inhA* expression was confirmed by construction of the *′mabA–inhA′–′lacZ* fusion, with and without the *mabA*^{g609a} mutation, with neither construct containing the native promoter region of the *mabA–inhA* operon. The level of *inhA–lacZ* expression was significantly higher using the construct with than without the g609a mutation, strongly supporting our hypothesis that a region adjacent to the g609a mutation in *mabA* acts as a promoter of *inhA* expression. Although silent mutations have not received attention as causes of drug resistance, the results of this study show that a silent mutation, especially one located upstream of drug-resistance genes, may be responsible for drug resistance. The *mabA*^{g609a} silent mutation is therefore a valuable marker of both INH and ETH resistance, as well as explaining INH resistance in certain strains of *Mtb*.

Experimental procedures

Growth conditions

Unless otherwise specified, bacterial strains were cultured as described (Ando *et al.*, 2011). When required for culturing mycobacteria and *Escherichia coli*, hygromycin (Wako) was added to concentrations of 75 and 150 μg ml^{-1} respectively; and kanamycin (Sigma) was added to concentrations of 20 and 50 μg ml^{-1} respectively. X-Gal (Sigma) was used at a concentration of 40 μg ml^{-1} for culturing mycobacteria.

Specialized transduction

The method used for specialized transduction has been described (Bardarov *et al.*, 2002; Vilcheze *et al.*, 2006). To construct a recombinant cosmid containing allelic exchange substrates, a 1000 bp DNA fragment containing *mabA*^{g609a} and *inhA* was amplified from a clinical isolate harbouring *mabA*^{g609a} using the primers AflII–*mabA*-F (5′-atgccttaagccg cgcgctggatgagcgga-3′, AflII site underlined) and *mabA*-R-XbaI (5′-atgctctagactagagcaattgggtgtgcg-3′, XbaI site underlined). The amplified DNA was digested with AflII and XbaI and cloned into the corresponding sites of pYUB854 (Bardarov *et al.*, 2002), resulting in the plasmid pYUB854::*mabA*^{g609a}–*inhA*. Subsequently, a 1057 bp DNA fragment containing *hemZ* was amplified using the primers BglII-*hemZ*-F (5′-ggaagatcttccatgcaatttgatgccgtcct-3′, BglII site underlined) and *hemZ*-SpeI-R (5′-gactagtctcacggcg atcctgcactcg-3′, SpeI site underlined), digested with BglII and SpeI, and cloned into the corresponding sites of pYUB854::*mabA*^{g609a}–*inhA*. The recombinant cosmid was

digested with PacI and ligated into the PacI treated shuttle phasmid phAE87 (Bardarov *et al.*, 2002). The resulting phasmid was packaged *in vitro* with Gigapack III (Stratagene) and used to transduce *E. coli* Stbl2 (Invitrogen). Phasmid was isolated and electroporated into *M. smegmatis* mc^2155, and the resulting transducing phage was amplified to obtain high-titer phage lysates. Ten millilitres of the *Mtb* H37Rv strain grown to log-phase were centrifuged, washed twice with Middlebrook 7H9 media (BD) supplemented with 10% ADC (BD) (7H9-ADC) and incubated for 22 h at 37°C. The bacterial culture was centrifuged and suspended in 500 µl of 7H9-ADC. Six microlitres of 100 mM $CaCl_2$ and 100 µl of high-titre phage lysate were added to the bacterial suspension and incubated for 3 h at 37°C; 3 ml 7H9-ADC were added, and the suspension was further incubated for 22 h at 37°C. After centrifugation, the bacteria were suspended in 400 µl 7H9-ADC and spread onto Middlebrook 7H10-OADC plates supplemented with 10% OADC (BD) containing hygromycin. The plates were incubated at 37°C.

Confirmation of correct chromosomal structures of isogenic strains

To analyse the chromosomal structures and the g609a mutation in isogenic strains, PCR, Southern blotting, and DNA sequencing were performed. For PCR, we used –200*mabA* (5′-ttcgtagggcgtcaatacac-3′) and *hemZ*+240-R (5′-agccccgtg gcctcgtcgagcagttgctcgaatcgtcacg-3′) primers, which bind upstream to *mabA* and downstream to *hemZ* respectively. Each reaction mixture contained 2× PrimeSTAR Max Premix (Takara), 0.25 mM of each primer, 20 ng of genomic DNA, and sterile distilled water to 50 µl. The amplification protocol consisted of 30 cycles of denaturation at 98°C for 10 s, annealing at 59°C for 5 s, and extension at 72°C for 1 min. These primers amplified a 3.0 kbp DNA fragment in H37Rv (Fig. 1B, lane 1), and a 5.0 kbp fragment in the isogenic strains that included a hygromycin resistance cassette (Fig. 1B, lanes 2–5). The identity of the PCR products was verified by direct DNA sequencing. Southern blotting was performed as described (Otsuka *et al.*, 2004). Genomic DNA was digested with BclI, electrophoresed on agarose gels, and detected using a *mabA–inhA* probe that had been amplified using the primers –200*mabA* and *inhA*+40 (5′-ccgaacga cagcagcaggac-3′). BclI-digested genomic DNA was incubated with horseradish peroxidase (HRP)-labelled *mabA–inhA* probe and visualized using SuperSignal West Femto Maximum Sensitivity Substrate (Thermo Scientific). BclI sites were located upstream of *mabA* and downstream of *hemZ*, not within *mabA–inhA*, *hemZ*, or the hygromycin resistance cassette. The probe detected a 6.6 kbp band in H37Rv (Fig. 1C, lane 1), and an 8.6 kbp band in the isogenic strains that included the hygromycin resistance cassette (Fig. 1C, lanes 2–5).

Drug susceptibility testing

Strains were tested for susceptibility to INH and ETH using an agar proportion method with 7H10-OADC plates according to the protocol of the Clinical Laboratory Standards Institute (NCCLS, 2003). We used the following drug concentrations: INH (0, 0.05, 0.1, 0.2, 0.3, 0.4, 0.5, 1.0 µg ml^{-1}) and ETH (0, 0.5, 1, 2, 4, 8, 16, 32, 64, 128, 256 µg ml^{-1}). The plates were incubated at 37°C for 3 weeks.

Preparation of total protein extracts

Proteins were extracted from bacterial cells as described (Ando *et al.*, 2011), with slight modifications, including disrupting the bacterial cells with Zirconia Beads (Ambion) and quantifying the protein concentrations of the extracts using Pierce BCA Protein Assay Kits (Thermo Scientific).

Preparation of anti-InhA polyclonal antibody

The coding region of *inhA*, without the start codon, was PCR amplified using the primers KpnI–*inhA* (5′-cggggtaccac aggactgctggacggcaaac-3′; KpnI site underlined) and *inhA*-HindIII (5′-cccaagcttctagagcaattgggtgtgcgc-3′; HindIII site underlined), digested with KpnI and HindIII, and cloned into the corresponding sites of pQE-2 (Invitrogen). All expressed proteins had N-terminal hexa-histidine residues. Purified 6× His-InhA was injected into a male Japanese white rabbit to raise polyclonal antibodies against InhA, with the antiserum used for Western blotting.

Western blotting

Western blotting was performed as described (Ando *et al.*, 2011). PVDF membranes were incubated with anti-HSP70 monoclonal antibody (1:500; Santa Cruz Biotechnology), followed by incubation with HRP-conjugated goat anti-mouse IgG (1:1000; Santa Cruz Biotechnology). Proteins were visualized using SuperSignal West Femto Maximum Sensitivity Substrate. Anti-HSP70 antibody was removed using WB Stripping Solution (nacalai tesque), and the membranes were incubated simultaneously with anti-InhA (diluted 1:20 000) and anti-KatG (diluted 1:10 000) polyclonal antibodies (Sekiguchi *et al.*, 2007), followed by incubation with HRP-conjugated donkey anti-rabbit IgG (1:10 000; GE Healthcare). Proteins were detected as described above.

Extraction of total RNA

Harvested bacterial cells were incubated with 900 µl TRIzol (Ambion) and 70 mg of Zirconia Beads, and the cells were disrupted by shaking in a FastPrep FP100A homogenizer (Savant; speed; 6.5; time; 30 s, three times). Bacterial lysates were treated with BCP Phase Separation Reagent (Molecular Research Center), and the aqueous phase was collected. Total RNA was extracted and cleaned using RNeasy Mini Kits (Qiagen) with on-column DNase treatment.

qRT-PCR

First-strand cDNA was synthesized with SuperScript III Reverse Transcriptase and random 6 mer primers (Invitrogen). The primer sets used to detect *mabA*, *inhA* and *sigA* were Rtime–*mabA*-F/Rtime–*mabA*-R (5′-ggatgaccgaggaaa agttc-3′/5′-tgccgatgccccagctgccg-3′), Rtime–*inhA*-F/Rtime–

inhA-R (5′-tatgcttcgatggccaaggc-3′/5′-cgccacgaacctgttgac cg-3′), and *sigA*-F/*sigA*-R (5′-atgacgacgaggagatcgctga-3′/5′-tttgaggtaggcgcgaaccgag-3′) respectively. qRT-PCR was performed on the Lightcycler 1.5 (Roche) with QuantiTect SYBR Green PCR Kits (Qiagen). The thermal cycling conditions included an initial denaturation at 95°C for 15 min, followed by 40 cycles of denaturation at 98°C for 30 s, annealing at 54°C for 1 min, and extension at 72°C for 30 s. Fluorescence was measured during each extension step.

RNA-seq

The rRNA was removed from each total RNA sample using Ribo-Zero rRNA Removal Kits (Gram-Positive Bacteria) (epicentre) and double-stranded cDNA was synthesized with cDNA Synthesis Kits (M-MLV Version) and random 9 mer primers (Takara). The cDNA libraries were prepared using Nextera DNA Sample Preparation kits (Illumina), according to the manufacturer's instructions. For multiplexing, the dual index system of the kit was employed. The resulting cDNA library products were sequenced using the MiSeq (Illumina) with a 300- or 500-cycle reagent kit to obtain 151×2 or 251×2 paired end reads. These paired end reads were mapped to the genome sequence of H37Rv (AL123456), and reads per kilobase of exon per million mapped reads (RPKM) (Mortazavi *et al.*, 2008) were calculated to obtain the normalized expression index of each gene using CLC genomics workbench (CLC bio). The RPKM values were used for volcano plot analysis (Cui and Churchill, 2003) to identify genes showing significantly different expression. Fold-change compared with H37Rv was calculated by Kal's test (Kal *et al.*, 1999). Transcription initiation sites were determined by contiguous expression, with each base supported by at least 10 uniquely mapped reads, a length of 100 bp and paired-end information.

β-Galactosidase assay

The plasmid pJEM13 (Timm *et al.*, 1994), carrying the *mabA*^{g609a}*–inhA′–′lacZ* fusion gene, was used to measure β-galactosidase activity in *Mtb* H37Rv. The plasmid contained a 479 bp DNA fragment, from nucleotide 409 of *mabA* to nucleotide 99 of *inhA*. A DNA fragment with or without the mutation was amplified using the primers ApaI–*mabA*-F (5′-acgcgggcccttcataggttcggtctccgg-3′, ApaI site underlined) and *inhA*-KpnI-R (5′-gcggggtaccgccctgctcctgggctaccc-3′, KpnI site underlined), digested with ApaI and KpnI, and cloned into the corresponding sites of pJEM13. These plasmids were used to transform H37Rv, and β-galactosidase activity was measured as described (Alland *et al.*, 2000). In addition, the transformants were streaked onto plates containing X-Gal to monitor *lacZ* expression visually.

Acknowledgements

We thank B. Gicquel for providing pJEM13; W.R. Jacobs, Jr for providing pYUB854 and phAE87; F. Kirikae for performing DST; and M. Komiya and Y. Sakurai for performing RNA-seq. This study was supported by a Grant for International Health Research (GIHR) (24A103) from the Ministry of Health, Labour and Welfare of Japan (MHLW), a grant from MHLW (H24-Shinko-Ippan-010), and a Grant-in-Aid for Scientific Research (C) (22590411) from the Ministry of Education, Culture, Sports, Science and Technology (MEXT) to T.K.; a GIHR (24A103) from MHLW to T.M.-A.; and a Grant-in-Aid for Young Scientists (B) (22790423) from MEXT to H.A.

Conflicts of interest

The authors declare no conflicts of interest.

References

Alland, D., Steyn, A.J., Weisbrod, T., Aldrich, K., and Jacobs, W.R., Jr (2000) Characterization of the *Mycobacterium tuberculosis iniBAC* promoter, a promoter that responds to cell wall biosynthesis inhibition. *J Bacteriol* **182:** 1802–1811.

Ando, H., Kondo, Y., Suetake, T., Toyota, E., Kato, S., Mori, T., and Kirikae, T. (2010) Identification of *katG* mutations associated with high-level isoniazid resistance in *Mycobacterium tuberculosis*. *Antimicrob Agents Chemother* **54:** 1793–1799.

Ando, H., Kitao, T., Miyoshi-Akiyama, T., Kato, S., Mori, T., and Kirikae, T. (2011) Downregulation of *katG* expression is associated with isoniazid resistance in *Mycobacterium tuberculosis*. *Mol Microbiol* **79:** 1615–1628.

Banerjee, A., Dubnau, E., Quemard, A., Balasubramanian, V., Um, K.S., Wilson, T., *et al.* (1994) *inhA*, a gene encoding a target for isoniazid and ethionamide in *Mycobacterium tuberculosis*. *Science* **263:** 227–230.

Banerjee, A., Sugantino, M., Sacchettini, J.C., and Jacobs, W.R. (1998) The *mabA* gene from the *inhA* operon of *Mycobacterium tuberculosis* encodes a 3-ketoacyl reductase that fails to confer isoniazid resistance. *Microbiology* **144** (Pt 10): 2697–2704.

Bardarov, S., Bardarov, S. Jr, Pavelka, M.S. Jr, Sambandamurthy, V., Larsen, M., Tufariello, J., *et al.* (2002) Specialized transduction: an efficient method for generating marked and unmarked targeted gene disruptions in *Mycobacterium tuberculosis*, *M. bovis* BCG and *M. smegmatis*. *Microbiology* **148:** 3007–3017.

Bernstein, J., Lott, W.A., Steinberg, B.A., and Yale, H.L. (1952) Chemotherapy of experimental tuberculosis. V. Isonicotinic acid hydrazide (nydrazid) and related compounds. *Am Rev Tuberc* **65:** 357–364.

Buchmeier, N.A., Newton, G.L., Koledin, T., and Fahey, R.C. (2003) Association of mycothiol with protection of *Mycobacterium tuberculosis* from toxic oxidants and antibiotics. *Mol Microbiol* **47:** 1723–1732.

Cui, X., and Churchill, G.A. (2003) Statistical tests for differential expression in cDNA microarray experiments. *Genome Biol* **4:** 210.

Espinal, M.A., Laszlo, A., Simonsen, L., Boulahbal, F., Kim, S.J., Reniero, A., *et al.* (2001) Global trends in resistance to antituberculosis drugs. World Health Organization-International Union against Tuberculosis and Lung Disease Working Group on Anti-Tuberculosis Drug Resistance Surveillance. *N Engl J Med* **344:** 1294–1303.

Hazbon, M.H., Brimacombe, M., Bobadilla del Valle, M., Cavatore, M., Guerrero, M.I., Varma-Basil, M., *et al.* (2006)

Population genetics study of isoniazid resistance mutations and evolution of multidrug-resistant *Mycobacterium tuberculosis*. *Antimicrob Agents Chemother* **50:** 2640–2649.

Heym, B., Stavropoulos, E., Honore, N., Domenech, P., Saint-Joanis, B., Wilson, T.M., *et al.* (1997) Effects of overexpression of the alkyl hydroperoxide reductase AhpC on the virulence and isoniazid resistance of *Mycobacterium tuberculosis*. *Infect Immun* **65:** 1395–1401.

Kal, A.J., van Zonneveld, A.J., Benes, V., van den Berg, M., Koerkamp, M.G., Albermann, K., *et al.* (1999) Dynamics of gene expression revealed by comparison of serial analysis of gene expression transcript profiles from yeast grown on two different carbon sources. *Mol Biol Cell* **10:** 1859–1872.

Larsen, M.H., Vilcheze, C., Kremer, L., Besra, G.S., Parsons, L., Salfinger, M., *et al.* (2002) Overexpression of *inhA*, but not *kasA*, confers resistance to isoniazid and ethionamide in *Mycobacterium smegmatis, M. bovis* BCG and *M. tuberculosis*. *Mol Microbiol* **46:** 453–466.

Lee, J.H., Ammerman, N.C., Nolan, S., Geiman, D.E., Lun, S., Guo, H., and Bishai, W.R. (2012) Isoniazid resistance without a loss of fitness in *Mycobacterium tuberculosis*. *Nat Commun* **3:** 753.

Mitarai, S., Kato, S., Ogata, H., Aono, A., Chikamatsu, K., Mizuno, K., *et al.* (2012) Comprehensive multicenter evaluation of a new line probe assay kit for identification of *Mycobacterium* species and detection of drug-resistant *Mycobacterium tuberculosis*. *J Clin Microbiol* **50:** 884–890.

Mortazavi, A., Williams, B.A., McCue, K., Schaeffer, L., and Wold, B. (2008) Mapping and quantifying mammalian transcriptomes by RNA-Seq. *Nat Methods* **5:** 621–628.

Otsuka, Y., Parniewski, P., Zwolska, Z., Kai, M., Fujino, T., Kirikae, F., *et al.* (2004) Characterization of a trinucleotide repeat sequence (CGG)5 and potential use in restriction fragment length polymorphism typing of *Mycobacterium tuberculosis*. *J Clin Microbiol* **42:** 3538–3548.

Ramaswamy, S., and Musser, J.M. (1998) Molecular genetic basis of antimicrobial agent resistance in *Mycobacterium tuberculosis*: 1998 update. *Tuber Lung Dis* **79:** 3–29.

Ramaswamy, S.V., Reich, R., Dou, S.J., Jasperse, L., Pan, X., Wanger, A., *et al.* (2003) Single nucleotide polymorphisms in genes associated with isoniazid resistance in *Mycobacterium tuberculosis*. *Antimicrob Agents Chemother* **47:** 1241–1250.

Ramaswamy, S.V., Dou, S.J., Rendon, A., Yang, Z., Cave, M.D., and Graviss, E.A. (2004) Genotypic analysis of multidrug-resistant *Mycobacterium tuberculosis* isolates from Monterrey, Mexico. *J Med Microbiol* **53:** 107–113.

Rozwarski, D.A., Grant, G.A., Barton, D.H., Jacobs, W.R., Jr, and Sacchettini, J.C. (1998) Modification of the NADH of the isoniazid target (InhA) from *Mycobacterium tuberculosis*. *Science* **279:** 98–102.

Sekiguchi, J., Miyoshi-Akiyama, T., Augustynowicz-Kopec, E., Zwolska, Z., Kirikae, F., Toyota, E., *et al.* (2007) Detection of multidrug resistance in *Mycobacterium tuberculosis*. *J Clin Microbiol* **45:** 179–192.

Timm, J., Lim, E.M., and Gicquel, B. (1994) *Escherichia coli*-mycobacteria shuttle vectors for operon and gene fusions to *lacZ*: the pJEM series. *J Bacteriol* **176:** 6749–6753.

Vilcheze, C., Weisbrod, T.R., Chen, B., Kremer, L., Hazbon, M.H., Wang, F., *et al.* (2005) Altered NADH/NAD^+ ratio mediates coresistance to isoniazid and ethionamide in mycobacteria. *Antimicrob Agents Chemother* **49:** 708–720.

Vilcheze, C., Wang, F., Arai, M., Hazbon, M.H., Colangeli, R., Kremer, L., *et al.* (2006) Transfer of a point mutation in *Mycobacterium tuberculosis inhA* resolves the target of isoniazid. *Nat Med* **12:** 1027–1029.

Vilcheze, C., Av-Gay, Y., Attarian, R., Liu, Z., Hazbon, M.H., Colangeli, R., *et al.* (2008) Mycothiol biosynthesis is essential for ethionamide susceptibility in *Mycobacterium tuberculosis*. *Mol Microbiol* **69:** 1316–1329.

Vilcheze, C., Av-Gay, Y., Barnes, S.W., Larsen, M.H., Walker, J.R., Glynne, R.J., and Jacobs, W.R., Jr (2011) Coresistance to isoniazid and ethionamide maps to mycothiol biosynthetic genes in *Mycobacterium bovis*. *Antimicrob Agents Chemother* **55:** 4422–4423.

Wang, F., Jain, P., Gulten, G., Liu, Z., Feng, Y., Ganesula, K., *et al.* (2010) *Mycobacterium tuberculosis* dihydrofolate reductase is not a target relevant to the antitubercular activity of isoniazid. *Antimicrob Agents Chemother* **54:** 3776–3782.

World Health Organization (2013) *Global Tuberculosis Report 2013*. Geneva: WHO Press.

Zhang, M., Yue, J., Yang, Y.P., Zhang, H.M., Lei, J.Q., Jin, R.L., *et al.* (2005) Detection of mutations associated with isoniazid resistance in *Mycobacterium tuberculosis* isolates from China. *J Clin Microbiol* **43:** 5477–5482.

Zhang, Y., and Yew, W.W. (2009) Mechanisms of drug resistance in *Mycobacterium tuberculosis*. *Int J Tuberc Lung Dis* **13:** 1320–1330.

Zhang, Y., Heym, B., Allen, B., Young, D., and Cole, S. (1992) The catalase-peroxidase gene and isoniazid resistance of *Mycobacterium tuberculosis*. *Nature* **358:** 591–593.

Infection, Genetics and Evolution 27 (2014) 294–299

Contents lists available at ScienceDirect

Infection, Genetics and Evolution

journal homepage: www.elsevier.com/locate/meegid

Dominant modern sublineages and a new modern sublineage of *Mycobacterium tuberculosis* Beijing family clinical isolates in Heilongjiang Province, China

Di Li [a], Cai-Bo Dong [a], Jia-Yi Cui [a], Chie Nakajima [b], Chun-Lei Zhang [c], Xin-Ling Pan [a], Gao-Xiang Sun [a], En-Yu Dai [d], Yasuhiko Suzuki [b], Min Zhuang [a], Hong Ling [a,*]

[a] *Department of Microbiology, Harbin Medical University, Heilongjiang Provincial Key Laboratory for Infection and Immunity, Key Laboratory of Etiology of Heilongjiang Province Education Bureau, Harbin, China*
[b] *Division of Global Epidemiology, Hokkaido University Research Center for Zoonosis Control, Sapporo, Hokkaido, Japan*
[c] *Harbin Chest Hospital, Harbin, China*
[d] *Department of Bioinformatics, Harbin Medical University, Harbin, China*

ARTICLE INFO

Article history:
Received 21 April 2014
Received in revised form 25 July 2014
Accepted 2 August 2014
Available online 8 August 2014

Keywords:
Mycobacterium tuberculosis
Beijing family
Single nucleotide polymorphism (SNP)
Evolution
Sublineage

ABSTRACT

Mycobacterium tuberculosis Beijing family includes a variety of sublineages. Knowledge of the distribution of a certain sublineage of the Beijing family may help to understand the mechanisms of its rapid spread and to establish an association between a certain genotype and the disease outcome. We have previously found that *M. tuberculosis* Beijing family clinical isolates represent approximately 90% of the clinical isolates from Heilongjiang Province, China. To clarify the distribution of *M. tuberculosis* Beijing family sublineages in Heilongjiang Province, China and to investigate the regularity rule for their evolution, we examined single nucleotide polymorphisms (SNPs) of 250 *M. tuberculosis* Beijing family clinical isolates using 10 SNP loci that have been identified as appropriate for defining Beijing sublineages. After determining the sequence type (ST) of each isolate, the sublineages of all *M. tuberculosis* Beijing family isolates were determined, and phylogenetic analysis was performed. We found that 9 out of the 10 SNP loci displayed polymorphisms, but locus 1548149 did not. In total, 92.8% of the isolates in Heilongjiang Province are modern sublineages. ST10 is the most prevalent sublineage (ST10 and ST22 accounted for 63.2% and 23.6% of all the Beijing family isolates, respectively). A new ST, accounting for 4% of the Beijing family isolates in this area, was found for the first time. Each new ST isolate showed a unique VNTR pattern, and none were clustered. The present findings suggest that controlling the spread of these modern sublineages is important in Heilongjiang Province and in China.

1. Introduction

The *Mycobacterium tuberculosis* (*M. tuberculosis*) Beijing family has spread widely in many countries and regions in the world (Bifani et al., 2002; Brudey et al., 2006; Hanekom et al., 2011) since it was first identified in 1995 (van Soolingen et al., 1995). Its wide spread has meant that great pressure has been brought to bear on the control of tuberculosis in China and world-wide. However, to date, the mechanisms for the rapid transmission of *M. tuberculosis* Beijing family are still unclear.

It has been claimed that *M. tuberculosis* Beijing family strains are resistant to Bacillus Calmette-Guerin (BCG) vaccination (Colditz et al., 1994; Parwati et al., 2010b), are highly virulent (Parwati et al., 2010a) and are associated with drug resistance (Almeida et al., 2005; Ghebremichael et al., 2010; Kremer et al., 2005; Tanveer et al., 2008). However, less association between this genotype and drug resistance has been reported in other geographic settings (Alonso et al., 2010; Anh et al., 2000; Jou et al., 2005; Toungoussova et al., 2003). An investigation regarding the epidemic of *M. tuberculosis* strains isolated in China revealed that Beijing family favors transmission but not drug resistance (Yang et al., 2012). We have also found that there is no difference in the drug resistance patterns between Beijing and non-Beijing genotype strains isolated in Heilongjiang Province, China, although the Beijing family represents approximately 90% of the clinical isolates in this area (Wang et al., 2011).

* Corresponding author. Present/permanent address: Department of Microbiology, Harbin Medical University, 194 Xuefu Road, Harbin 150081, Heilongjiang Province, China. Tel./fax: +86 0451 86685122.
E-mail address: lingh@ems.hrbmu.edu.cn (H. Ling).

http://dx.doi.org/10.1016/j.meegid.2014.08.004
1567-1348/

The Beijing family contains a variety of subfamilies or sublineages (Filliol et al., 2006). The significance of genotyping always provides insights for phenotype, disease outcome and sources of infection. Knowledge of the distribution features of a certain sublineage of the Beijing family may improve our understanding of the mechanisms of its rapid spread and establish an association between a certain genotype and disease outcome.

Single nucleotide polymorphisms (SNPs) are used for genetically classifying *M. tuberculosis* and identifying sublineages. Because horizontal gene transfer or genetic recombination among different strains of *M. tuberculosis* complex (MTBC) is rare, the changes in genetic information are almost always obtained though hereditary from parental strains (Baker et al., 2004; Huard et al., 2006; Stucki et al., 2012). Therefore, SNPs have been used to classify *M. tuberculosis* Beijing family into different sequence types (STs) and is considered to be a robust target for defining the accurate position of a certain strain in a phylogenetic tree (Chen et al., 2012; Faksri et al., 2011; Filliol et al., 2006; Iwamoto et al., 2012; Mestre et al., 2011; Nakanishi et al., 2013; Qiao et al., 2010; Wada et al., 2009b).

To date, ancient and modern sublineages have been identified by SNPs. Though modern STs are dominant, the trends in the distribution of certain sublineages are geographically variable (Chen et al., 2012; Filliol et al., 2006; Iwamoto et al., 2012). For instance, a modern sublineage, ST10, prevails in Chongming Island, Taiwan, Thailand, and Peru (Chen et al., 2012; Faksri et al., 2011; Iwamoto et al., 2012; Qiao et al., 2010), while an ancient type, ST19, is the dominant sublineage in Japan (Nakanishi et al., 2013; Wada et al., 2009b). However, the worldwide distribution and the epidemiological significance of the sublineages have not been well clarified yet. Extensive investigations regarding the possible reasons for the predominant prevalence of certain sublineages are needed to explore the significance of the variable distribution, the correlation between the evolution of *M. tuberculosis* Beijing family and its transmission patterns, and the impact on the spread of tuberculosis.

China is a country with a high burden of tuberculosis (TB). Heilongjiang Province, located in northeastern China, is one of the regions where the prevalence of both TB and drug-resistant TB is higher than the average level in China. We have found that *M. tuberculosis* Beijing family clinical isolates are the dominant TB strains in Heilongjiang Province (Wang et al., 2011). However, no correlation between the prevalence of Beijing family strains and general drug resistance has been found (Wang et al., 2011). It is urgent to understand possible mechanisms behind the spread of *M. tuberculosis*, especially drug-resistant strains.

In the present study, our aim was to discover the distribution features and proportions of *M. tuberculosis* Beijing family sublineages in Heilongjiang Province. We also aimed to define appropriate SNP loci for analyzing the sublineages of locally prevalent *M. tuberculosis* Beijing family clinical isolates. The findings will facilitate our understanding of the possible reasons for the predominant prevalence of certain sublineages and the highly epidemic of Beijing family in this area.

2. Materials and methods

2.1. M. tuberculosis clinical isolates

All the *M. tuberculosis* clinical strains were isolated from the patients from various regions of Heilongjiang province who were diagnosed with pulmonary TB at Harbin Chest Hospital. From June 2007 to November 2009, a total of 300 isolates were collected. Among them, 269 isolates were identified as *M. tuberculosis* Beijing family strains. Of these, 250 that had enough DNA for genotyping, including 60 from 2007, 107 from 2008, and 83 from 2009, were used in this study. *M. tuberculosis* H37Rv was used as the reference strain. All the patients were HIV-1 negative, and 68.4% (171/250) were male.

2.2. SNP typing

DNA extraction, molecular identification of *M. tuberculosis*, and the identification of Beijing family strains were carried out as described in our previous study (Wang et al., 2011).

The ten SNP loci shown in Table 1 were chosen because they have established polymorphisms among *M. tuberculosis* Beijing family strains and have been used for analyzing Beijing sublineages (Chen et al., 2012; Faksri et al., 2011; Iwamoto et al., 2012; Nakanishi et al., 2013; Qiao et al., 2010; Wada et al., 2009b). Polymerase chain reaction (PCR) amplification was carried out using the primers of Nakajima et al. (2013). Each PCR mixture was prepared in a volume of 50 μL containing 50 ng of genomic DNA, 2× Taq PCR Master Mix 25 μl (Nuo Weisen Biotech Co., Ltd., Beijing), and 0.2 μM of the corresponding primer. The PCR reactions were performed as follows: 75 °C for 5 min, 30 cycles of 75 °C for 10 s, 53 °C for 10 s, and 72 °C for 20 s, and final extension at 72 °C for 5 min. The PCR products were sequenced by Sangon Biotech (Shanghai) Co., Ltd. using the dideoxy chain termination method.

Nucleotide blast was carried out online (http://blast.ncbi.nlm.nih.gov/Blast.cgi), and any differences between clinical isolates and the sequence of the reference $H_{37}Rv$ genome were identified. STs were determined based on the database and as previously described elsewhere (Chen et al., 2012; Faksri et al., 2011; Iwamoto et al., 2012; Nakanishi et al., 2013; Qiao et al., 2010; Wada et al., 2009b).

2.3. Identification of modern/ancient Beijing strains

It has been found that all modern Beijing strains of *M. tuberculosis* carry a mutation in codon 58 of the mutT2 gene (Hanekom et al., 2007; Iwamoto et al., 2008; Luo et al., 2012). Thus, a part of the mutT2 gene containing codon 58 was amplified. The primers included MutT2-Mut, (AGAGCTCGCCGAAGAACCGC, Forward), MutT2-Wt, (AGAGCTCGCCGAAGAACCGG, Forward), and MutT2-r (AAGCAGATGCACGCGATAGG, Reverse). Each strain was amplified using two pairs of primers: MutT2-Mut/MutT2-r (positive amplification only from mutants) and MutT2-Wt/MutT2-r (positive amplification only from wild-type). Each PCR mixture was prepared in a volume of 20 μL containing 150 ng of genomic DNA, 2× Taq PCR Master Mix 12.5 μl (Nuo Weisen Biotech Co., Ltd.,

Table 1
SNP loci and the primers used in identifying the mutations.

Locus[a]	Nucleotide sequence	Product size (bp)
797736	Forward: GACGGCCGAATCTGACACTG	266
	Reverse: CCATTCCGGGTGGTCACTG	
909166	Forward: CGTCGAGCTCCCACTTCTTG	288
	Reverse: TCGTCGAAGTGGACGAGGAC	
1477596	Forward: GTCGACAGCGCCAGAAAATG	232
	Reverse: GCTCCTATGCCACCCAGCAC	
1548149	Forward: GGCCAAGCCGTGTATTAGGG	306
	Reverse: AGTCGGCAGTGACGTTCTCG	
1692069	Forward: GATTGGCAACTGGCAACAGG	332
	Reverse: TGGCCGTTTCAGATAGCACAC	
1892017	Forward: GCTGCACATCATGGGTTGG	278
	Reverse: GTATCGAGGCCGACGAAAGG	
2376135	Forward: TCTTGCGACCCGATGTGAAC	373
	Reverse: GAGCGCAACATGGGTGAGTC	
2532616	Forward: CCCTTTTCTGCTCGGACACG	278
	Reverse: GATCGACCTTCGTGCACTGG	
2825581	Forward: CCTTGGAGCGCAACAAGATG	306
	Reverse: CTGGCCGGACGATTTTGAAG	
4137829	Forward: CGTCGCTGCAATTGTCTGG	229
	Reverse: GGACGCAGTCGCAACAGTTC	

[a] Position of SNP locus in $H_{37}Rv$ genome.

Beijing), and 0.2 μM of each corresponding primer. The PCRs were performed as follows: 75 °C for 15 min, 35 cycles of 94 °C for 1 min, 70 °C for 1 min and 72 °C for 1 min, and a final extension at 72 °C for 10 min.

2.4. MIRU-VNTR analysis

To identify the VNTR profile of the *M. tuberculosis* isolates with new sequence types, we choose 14 of the 15 MIRU-VNTR loci that have been recommended for analyzing the VNTR profile of *M. tuberculosis* strains worldwide (Supply et al., 2006). One locus, ETR-C, was excluded because it displayed no discrimination power based our investigation (data not shown) and findings by others (Wang et al., 2011). The PCR conditions and the calculation of copy number were described previously (Wang et al., 2011). The dendrogram was drawn by Ward with the 14 selected VNTR locus results by BioNumerics version 6.6 (Applied Maths, Belgium).

3. Results

3.1. The polymorphism of M. tuberculosis Beijing family isolates and identification of the SNP loci

The 10 SNP loci we used in the present study have been widely used for identifying sublineage of *M. tuberculosis* Beijing family (Filliol et al., 2006). We found that the isolates from Heilongjiang Province displayed polymorphisms at 9 SNP loci. Locus 1548149 did not exhibit any polymorphism. Therefore, the other 9 loci were used for subsequent analyses of sublineage of the local epidemic isolates.

To identify the discrimination power of the 9 SNP loci for identifying the STs of the local epidemic Beijing family isolates, we first analyzed the usefulness of the 9-SNP-locus combination in determining STs. A combination of 8 loci (without locus 909166) was able to classify all of our Beijing family isolates into 7 groups: ST11/ST26, ST3, ST25/ST19, ST10/STF, ST-CH1, ST22, and ST8 (Table 2). Locus 909166 demonstrated an advantage in discriminating between ST11 and ST26, ST25 and ST19, and ST10 and STF.

We also established the evolutionary order of the sublineages, including the ancient and the modern sublineages (Table 2). ST-CH1 was located between ST10 and ST22, confirming that it evolved from ST10.

3.2. The prevalence of the sublineages of Beijing family strains

We found that ST10 and ST22 were the most prevalent STs among the *M. tuberculosis* Beijing family isolates in Heilongjiang Province (Table 2). ST10 and ST22 accounted for 86.8% of all the Beijing family isolates, at 63.2% and 23.6%, respectively, indicating that ST10 is the most predominant sublineage in this region.

A new ST, found at 4% (10 isolates) of all the local epidemic Beijing family isolates, was found in this region. The new mutation pattern of the 10 isolates belonging to this ST appeared at loci 2532616 and 2376135. This is the first record of this new ST, and we named it ST-CH1.

Subsequently, identification of modern/ancient sublineages was carried out. In total, 18 (7.2%) Beijing family *M. tuberculosis* clinical isolates were identified as ancient sublineages, including those belonging to ST11, ST26, ST3, ST25, and ST19. In contrast, 92.8% of the local epidemic isolates were modern sublineages.

We further analyzed the yearly distribution of the *M. tuberculosis* Beijing family strains in Heilongjiang Province. We found that ST10 and ST22 were also the predominant STs in 2007, 2008, and 2009. The three-year distribution of ST10 was 63.3%, 53.3% and 75.9%, respectively; while that of ST22 was 26.7%, 27.1%, and 16.9%, respectively (Table 3). In 2009, the percentage of ST10/STF was the highest and that of ST22 was the lowest. The distribution trends of other STs could not be estimated because of their low prevalence.

Overall, between 2007 and 2009, the modern sublineages accounted for 90.0%, 91.6%, and 96.4% of all the Beijing isolates; the ancient sublineages accounted for 10.0%, 8.4%, and 3.6%. The prevalence of the modern sublineages increased yearly.

3.3. VNTR profile of the ST-CH1 isolates

According to the VNTR profile of the 10 strains belonging to ST-CH1, each isolate showed a unique VNTR pattern, and none were clustered (Fig. 1). This phenomenon suggests that the emergence of ST-CH1 did not occur via an outbreak.

4. Discussion

Although *M. tuberculosis* is highly conserved compared to many other bacterial species, it still has some genetic diversity. SNPs among *M. tuberculosis* strains can not only be used to divide *M. tuberculosis* into different subtypes but are also considered as a

Table 2
Sequence types and the proportions of *M. tuberculosis* Beijing genotype isolates from Heilongjiang (n = 250).

ST[a]	SNPs									No. isolate (%)	Sublineage
	797736	2825581	1892017	4137829	1477596	2532616	2376135	1692069			
ST11/ST26	C	T	T	C	C	G	A	A		7 (2.8)	Ancient
ST3	T	G	T	C	C	G	A	A		4 (1.6)	Ancient
ST25/ST19	T	G	C	T	C	G	A	A		7 (2.8)	Ancient
ST10/STF	T	G	C	T	T	G	A	A		162 (64.8)	Modern
ST-CH1[b]	T	G	C	T	T	A	A	A		10 (4.0)	Modern
ST22	T	G	C	T	T	A	G	A		59 (23.6)	Modern
ST8	T	G	C	T	T	A	G	G		1 (0.4)	Modern
	797736	2825581	1892017	4137829	1477596	2532616	2376135	1692069	909166		
ST11	C	T	T	C	C	G	A	A	C	2 (0.8)	Ancient
ST26	C	T	T	C	C	G	A	A	T	5 (2.0)	Ancient
ST3	T	G	T	C	C	G	A	A	C	4 (1.6)	Ancient
ST25	T	G	C	T	C	G	A	A	C	3 (1.2)	Ancient
ST19	T	G	C	T	C	G	A	A	T	4 (1.6)	Ancient
STF	T	G	C	T	T	G	A	A	C	4 (1.6)	Modern
ST10	T	G	C	T	T	G	A	A	T	158 (63.2)	Modern
ST-CH1[b]	T	G	C	T	T	A	A	A	T	10 (4.0)	Modern
ST22	T	G	C	T	T	A	G	A	T	59 (23.6)	Modern
ST8	T	G	C	T	T	A	G	G	T	1 (0.4)	Modern

[a] Sequence type.
[b] New ST found in present study.

Table 3
Yearly distributions of sublineages of Beijing family isolates in Heilongjiang from 2007 to 2009.

	No. of isolates	Beijing sublineages	STs	No. isolate (%)[a]
2007	60	Modern	ST10	38 (63.3)
			ST22	16 (26.7)
			Others	0
		Ancient		6 (10.0)
2008	107	Modern	ST10	57 (53.3)
			ST22	29 (27.1)
			Others	12 (11.2)
		Ancient		9 (8.4)
2009	83	Modern	ST10	63 (75.9)
			ST22	14 (16.9)
			Others	3(3.6)
		Ancient		3 (3.6)

[a] A rate represents the proportion of the isolates collected in the corresponding year.

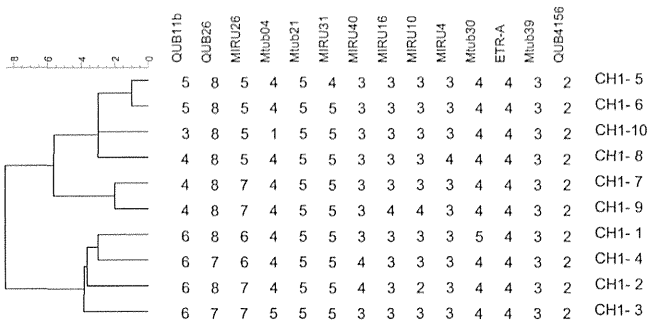

Fig. 1. VNTR patterns and the dendrogram of 10 ST-CH1 isolates. The dendrogram was drawn with the 14 selected MIRU-VNTR loci by using Ward of BioNumerics version 6.6 (Applied Maths, Belgium).

robust target for defining the accurate evolutionary lineage of a strain. Filliol et al. have found that a dendrogram drawn with SNPs most accurately reflects the true evolution of the *M. tuberculosis* complex and, furthermore, have found that some SNPs are specific to the Beijing family strains (Filliol et al., 2006).

Synonymous SNPs (sSNPs) are used to analyze the evolution of *M. tuberculosis* because the influence of evolutionary pressure can be avoided, meaning that they are more accurate tools for examining evolutionary history (Baker et al., 2004; Huard et al., 2006; Nakajima et al., 2013; Schork et al., 2000; Stucki et al., 2012). The 10 SNP loci identified by Filliol et al. are synonymous and have been used in defining the sublineages of Beijing family strains (Filliol et al., 2006; Hanekom et al., 2007; Iwamoto et al., 2008). However, more evidence that confirms their fitness in different geographic locations is still needed. Recently, it has been found that some SNP loci show geographically limited polymorphisms and are not suitable for global phylogenetic analysis (Faksri et al., 2011). For instance, locus 1548149 displays no polymorphisms among clinical isolates from Chongming Island, Shanghai, Japan and Thailand (Faksri et al., 2011; Iwamoto et al., 2008; Qiao et al., 2010), but it displays a polymorphism in Taiwan (Chen et al., 2012). Some researchers have also suggested excluding this locus because it does not represent unique, irreversible events (Faksri et al., 2011; Nakanishi et al., 2013). More comprehensive investigations using a large number of samples are still needed. In the present study, we found that locus 1548149 is not suitable for the classification of the *M. tuberculosis* Beijing family isolates that are epidemic in Heilongjiang Province because it displays no polymorphisms in these samples.

We also found that SNP 909166 displays a reversible polymorphism among the *M. tuberculosis* isolates in Heilongjiang Province. It has been confirmed that SNP 909166 plays a key role in classifying *M. tuberculosis* strains into the STK and ST3 sublineages that are predominant in Japan (Wada et al., 2009b). However, the polymorphism at this locus is reversible, and the robustness of the branches identified using SNP 909166 is relatively low (Nakanishi et al., 2013). Instead of this locus, locus 1576481 is suggested useful in evolutionary studies involving the discrimination of STK and ST3 because it is more reliable (Nakanishi et al., 2013). SNP 909166 plays a role in the discrimination between ST19 and ST25, ST11 and ST26, and STF and ST10; therefore, it is still useful for the discrimination of sublineages of *M. tuberculosis* clinical isolates in Heilongjiang Province. It is necessary to perform more analyses using a larger sample set and isolates from multiple geographic areas to find more unique and irreversible SNPs for epidemiological and evolution studies.

Clarifying the distribution of a certain Beijing family sublineage assists us in understanding the causative events for their rapid spread and helps us to establish an association between a certain genotype and the disease outcome. The high prevalence of the modern sublineage of the *M. tuberculosis* Beijing family has been found in Chongming Island, Shanghai, Taiwan of China, Thailand, and Peru (Table 4). The proportion of strains in Peru, South America that were the modern sublineage was 85.7% from 1999 to 2006 and increased to 93.9% in the years 2008–2010 (Iwamoto et al., 2012). Although the ancient sublineage still dominates in Japan, an increase in modern sublineages has occurred recently in the homeless population in Osaka City, Japan (Wada et al., 2009a). ST 10 is the dominant ST in Taiwan, China, where the prevalence is 53.3% (Table 4). Moreover, this sublineage is also dominant in Thailand (57.7%) (Faksri et al., 2011).

In Heilongjiang Province, two modern sublineages, ST10 and ST22, account for 86.8% of the Beijing family isolates. The consistently high prevalence from 2007 to 2009 implies stability to the predominance of the Beijing family in this area.

However, in a southern region of China, Chongming Island, Shanghai, a higher prevalence (30.4%) of ST19 has been found compared to that in Heilongjiang Province (1.6%) (Qiao et al., 2010). Actually, ST19 dominates in Japan and accounts for 31.3% of all Beijing family isolates (Wada et al., 2009b). The high prevalence of ST19 in both Japan and Chongming Island may suggest an active transmission between the two geographically close regions due to active reciprocal trade and tourism.

Moreover, one new modern ST (ST-CH1) was found in Heilongjiang Province. ST-CH1 evolved from ST10, and ST22 was branched off to form ST-CH1. Both of the offspring of ST10 and ST22 are currently dominant, but the majority of the progeny of ST-CH1 are already extinct. Usually, those extricated lineages have not spread globally. They evolved locally and remained local. This very rare "missing link" lineage still survives in Heilongjiang Province and accounts for approximately 4% of the local epidemic Beijing family isolates, suggesting that the evolution of ST10 to ST22 might occur around this area. ST-CH1 is a modern sublineage, the evolution of which occurred later than ST10 but earlier than ST22. The genetic distance is closer to ST10 than to ST22. We could not identify the origin of this ST or establish the significance of this ST in the evolution of *M. tuberculosis* Beijing family yet. However, the emergence of the strains is not from an outbreak of a single clone because the isolates have variable VNTR patterns.

There are two new STs that account for 3.0% (ancient sublineage) and 1.5% (modern sublineage) of Beijing family strains isolated in Chongming Island, Shanghai (Qiao et al., 2010). These STs are different from ST-CH1, found in Heilongjiang Province.

In the evolutionary history of a species, mutations in SNPs occur one by one. However, some intermediate types have already disappeared, and we are unable to know which mutation occurred first, for example, between SNP 797736 and 2825581and between SNP

Table 4
Distribution features of STs of Beijing *M. tuberculosis* isolates from different areas.

ST[a]	Heilongjiang Province (present study)	Chongming Island (Qiao et al., 2010)	Taiwan (Chen et al., 2012)	Japan (Wada et al., 2009b)	Thailand (Faksri et al., 2011)	Peru (Iwamoto et al., 2012)
ST11	2 (0.8)		4 (1.2)	4 (1.1)	3 (1.8)	
ST26	5 (2.0)	10 (7.4)	27 (8.0)	28 (7.9)		4 (1.5)
ST3	4 (1.6)	1 (0.7)	13 (3.8)	84 (23.7)		4 (1.5)
STK			4 (1.2)	51 (14.4)	3 (1.8)	
ST19	4 (1.6)	41 (30.4)	50 (14.8)	111 (31.3)	28 (17.2)	13 (4.9)
ST25	3 (1.2)	1 (0.7)	7 (2.1)	2 (0.6)		1 (0.3)
ST22	59 (23.6)	19 (14.1)	49 (14.5)	14 (3.9)	28 (17.2)	15 (5.6)
ST10	158 (63.2)	57 (42.2)	180 (53.3)	61 (17.2)	94 (57.7)	231 (86.2)
ST8	1(0.4)				5 (3.1)	
STN			4 (1.2)			
STF	4 (1.6)				2 (1.2)	
ST-CH1[b]	10 (4.0)					
NEW1[c]		4 (3.0)				
NEW2[c]		2 (1.5)				
Total	250	135	338	355	163	268

[a] Sequence type.
[b] New ST found in Heilongjiang Province.
[c] New STs found in Chongming Island, Shanghai.

2532616 and 2376135. The SNPs of ST-CH1 at these loci indicate that the SNP 2532616 mutation was earlier than 2376135.

Despite the small number of ST8 isolates, it is the most recently evolved modern sublineage and is rarely found in other areas (Faksri et al., 2011).

In conclusion, we defined a SNP locus set (a 9-locus combination) that is suitable for the differentiation of polymorphisms of Beijing family isolates in Heilongjiang Province. Furthermore, a new modern ST, the ancestor of ST22, has been identified for the first time, and we established that the strains of the new ST are not originally from an outbreak. Moreover, in this area, more than 90% of the Beijing family strains are of modern sublineages, especially the predominant sublineages ST10 and ST22, which contribute to the high prevalence of the Beijing family in this region. Hence, extensive investigation of the phenotypes of the isolates of these modern STs will aid in our understanding of the rapid transmission of Beijing family strains. Monitoring evolutionary dynamics can also predict the epidemic trends of *M. tuberculosis* in a local region, as well as throughout China, because rapid evolution may promote the occurrence of new types or subtypes of the species. Understanding the phylogeny of new types of *M. tuberculosis* can improve studies of pathogenicity, host specificity, virulence determinants, host adaptation, and epidemic potential. Here, we provide a basis for the statement that controlling the spread of these modern sublineages will be important for decreasing the disease prevalence caused by these sublineages in Heilongjiang Province and in China.

Acknowledgement

We thank Li-Na Zhao and Bo Wang at Harbin Chest Hospital for assistance in collecting *M. tuberculosis* isolates. We are grateful to Dr. Hattori T at Tohoku University, Japan, for the helpful and scientific discussion about bacterium evolution. The work was supported by the grant for graduate program from Harbin medical University to Dong CB, Cui JY.

References

Almeida, D., Rodrigues, C., Ashavaid, T.F., Lalvani, A., Udwadia, Z.F., Mehta, A., 2005. High incidence of the Beijing genotype among multidrug-resistant isolates of *Mycobacterium tuberculosis* in a tertiary care center in Mumbai, India. Clin. Infect. Dis. 40, 881–886.

Alonso, M., Alonso Rodríguez, N., Garzelli, C., Martinez Lirola, M., Herranz, M., Samper, S., Ruiz Serrano, M.J., Bouza, E., Garcia de Viedma, D., 2010. Characterization of *Mycobacterium tuberculosis* Beijing isolates from the Mediterranean area. BMC Microbiol. 10, 151.

Anh, D.D., Borgdorff, M.W., Van, L.N., Lan, N.T., van Gorkom, T., Kremer, K., van Soolingen, D., 2000. *Mycobacterium tuberculosis* Beijing genotype emerging in Vietnam. Emerg. Infect. Dis. 6, 302–305.

Baker, L., Brown, T., Maiden, M.C., Drobniewski, F., 2004. Silent nucleotide polymorphisms and a phylogeny for *Mycobacterium tuberculosis*. Emerg. Infect. Dis. 10, 1568–1577.

Bifani, P.J., Mathema, B., Kurepina, N.E., Kreiswirth, B.N., 2002. Global dissemination of the *Mycobacterium tuberculosis* W-Beijing family strains. Trends Microbiol. 10, 45–52.

Brudey, K., Driscoll, J.R., Rigouts, L., Prodinger, W.M., Gori, A., Al-Hajoj, S.A., Allix, C., Aristimuno, L., Arora, J., Baumanis, V., Binder, L., Cafrune, P., Cataldi, A., Cheong, S., Diel, R., Ellermeier, C., Evans, J.T., Fauville-Dufaux, M., Ferdinand, S., Garcia de Viedma, D., Garzelli, C., Gazzola, L., Gomes, H.M., Guttierez, M.C., Hawkey, P.M., van Helden, P.D., Kadival, G.V., Kreiswirth, B.N., Kremer, K., Kubin, M., Kulkarni, S.P., Liens, B., Lillebaek, T., Ho, M.L., Martin, C., Martin, C., Mokrousov, I., Narvskaia, O., Ngeow, Y.F., Naumann, L., Niemann, S., Parwati, I., Rahim, Z., Rasolofo-Razanamparany, V., Rasolonavalona, T., Rossetti, M.L., Rusch-Gerdes, S., Sajduda, A., Samper, S., Shemyakin, I.G., Singh, U.B., Somoskovi, A., Skuce, R.A., van Soolingen, D., Streicher, E.M., Suffys, P.N., Tortoli, E., Tracevska, T., Vincent, V., Victor, T.C., Warren, R.M., Yap, S.F., Zaman, K., Portaels, F., Rastogi, N., Sola, C., 2006. *Mycobacterium tuberculosis* complex genetic diversity: mining the fourth international spoligotyping database (SpolDB4) for classification, population genetics and epidemiology. BMC Microbiol. 6, 23.

Chen, Y.Y., Chang, J.R., Huang, W.F., Kuo, S.C., Su, I.J., Sun, J.R., Chiueh, T.S., Huang, T.S., Chen, Y.S., Dou, H.Y., 2012. Genetic diversity of the *Mycobacterium tuberculosis* Beijing family based on SNP and VNTR typing profiles in Asian countries. PLoS ONE 7, e39792.

Colditz, G.A., Brewer, T.F., Berkey, C.S., Wilson, M.E., Burdick, E., Fineberg, H.V., Mosteller, F., 1994. Efficacy of BCG vaccine in the prevention of tuberculosis. Meta-analysis of the published literature. J. Am. Med. Assoc. 271, 698–702.

Faksri, K., Drobniewski, F., Nikolayevskyy, V., Brown, T., Prammananan, T., Palittapongarnpim, P., Prayoonwiwat, N., Chaiprasert, A., 2011. Genetic diversity of the *Mycobacterium tuberculosis* Beijing family based on IS6110, SNP, LSP and VNTR profiles from Thailand. Infect. Genet. Evol. 11, 1142–1149.

Filliol, I., Motiwala, A.S., Cavatore, M., Qi, W., Hazbon, M.H., Bobadilla del Valle, M., Fyfe, J., Garcia-Garcia, L., Rastogi, N., Sola, C., Zozio, T., Guerrero, M.I., Leon, C.I., Crabtree, J., Angiuoli, S., Eisenach, K.D., Durmaz, R., Joloba, M.L., Rendon, A., Sifuentes-Osornio, J., Ponce de Leon, A., Cave, M.D., Fleischmann, R., Whittam, T.S., Alland, D., 2006. Global phylogeny of *Mycobacterium tuberculosis* based on single nucleotide polymorphism (SNP) analysis: insights into tuberculosis evolution, phylogenetic accuracy of other DNA fingerprinting systems, and recommendations for a minimal standard SNP set. J. Bacteriol. 188, 759–772.

Ghebremichael, S., Groenheit, R., Pennhag, A., Koivula, T., Andersson, E., Bruchfeld, J., Hoffner, S., Romanus, V., Kallenius, G., 2010. Drug resistant *Mycobacterium tuberculosis* of the Beijing genotype does not spread in Sweden. PLoS ONE 5, e10893.

Hanekom, M., Gey van Pittius, N.C., McEvoy, C., Victor, T.C., Van Helden, P.D., Warren, R.M., 2011. *Mycobacterium tuberculosis* Beijing genotype: a template for success. Tuberculosis 91, 510–523.

Hanekom, M., van der Spuy, G.D., Streicher, E., Ndabambi, S.L., McEvoy, C.R., Kidd, M., Beyers, N., Victor, T.C., van Helden, P.D., Warren, R.M., 2007. A recently evolved sublineage of the *Mycobacterium tuberculosis* Beijing strain family is associated with an increased ability to spread and cause disease. J. Clin. Microbiol. 45, 1483–1490.